iScience

CellPress

Article

Phosphorylation Alters the Properties of Pol η: Implications for Translesion Synthesis

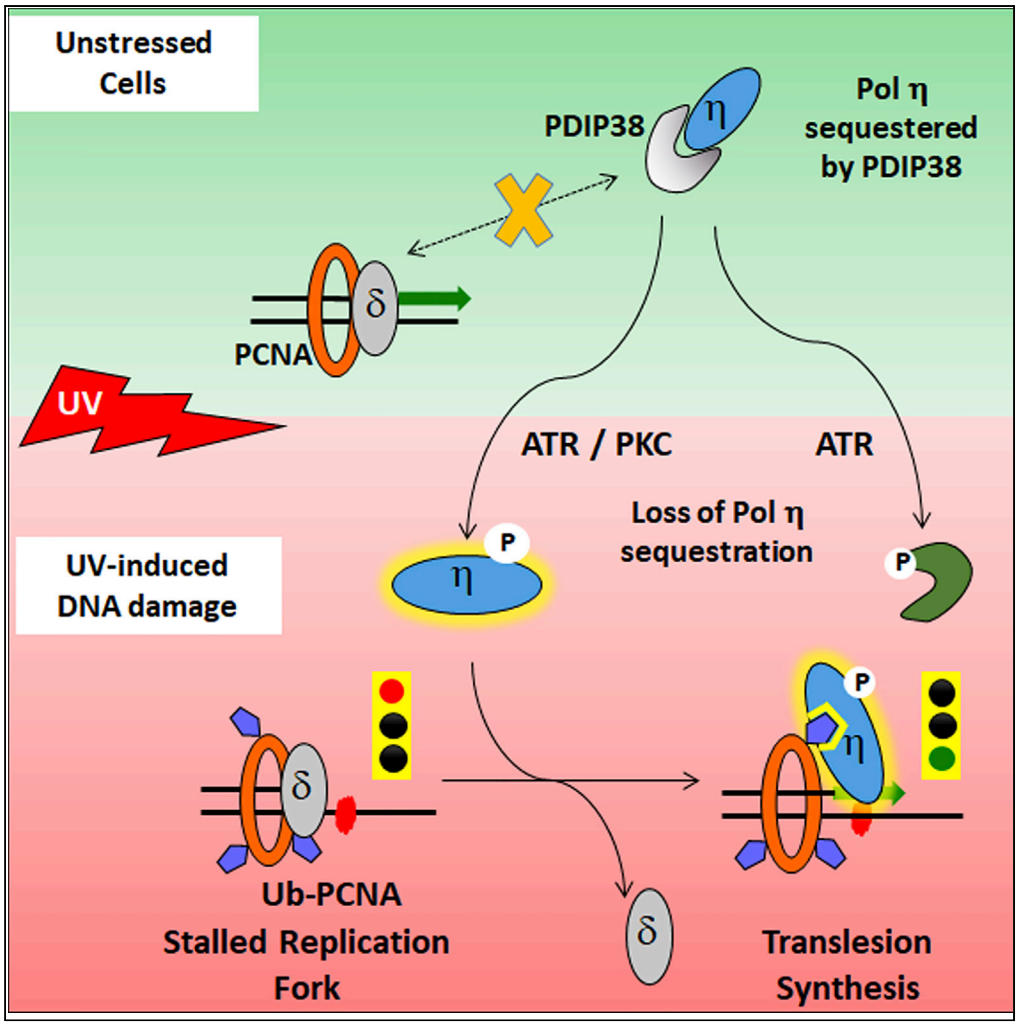

Chandana Peddu, Sufang Zhang, Hong Zhao, Agnes Wong, Ernest Y.C. Lee, Marietta Y.W.T. Lee, Zhongtao Zhang

zhongtao_zhang@nymc.edu

HIGHLIGHTS

Pol η activation requires both ATR and PKC phosphorylation

Phosphorylation directly enhances the affinity of Pol η toward Ub-PCNA

PDIP38 sequesters Pol η away from normal replication fork

Pol δ is not able to displace phosphorylated Pol η from Ub-PCNA complex

Peddu et al., iScience 6, 52–67
August 31, 2018
https://doi.org/10.1016/j.isci.2018.07.009

iScience

CellPress

Article

Phosphorylation Alters the Properties of Pol η: Implications for Translesion Synthesis

Chandana Peddu,[1] Sufang Zhang,[1] Hong Zhao,[2] Agnes Wong,[1,3] Ernest Y.C. Lee,[1] Marietta Y.W.T. Lee,[1] and Zhongtao Zhang[1,4,*]

SUMMARY

There are significant ambiguities regarding how DNA polymerase η is recruited to DNA lesion sites in stressed cells while avoiding normal replication forks in non-stressed cells. Even less is known about the mechanisms responsible for Pol η-induced mutations in cancer genomes. We show that there are two safeguards to prevent Pol η from adventitious participation in normal DNA replication. These include sequestration by a partner protein and low basal activity. Upon cellular UV irradiation, phosphorylation enables Pol η to be released from sequestration by PDIP38 and activates its polymerase function through increased affinity toward monoubiquitinated proliferating cell nuclear antigen (Ub-PCNA). Moreover, the high-affinity binding of phosphorylated Pol η to Ub-PCNA limits its subsequent displacement by Pol δ. Consequently, activated Pol η replicates DNA beyond the lesion site and potentially introduces clusters of mutations due to its low fidelity. This mechanism could account for the prevalence of Pol η signatures in cancer genome.

INTRODUCTION

In non-stressed cells, the exclusive participation of high-fidelity DNA polymerases (Pol δ and Pol ε) in routine DNA replication processes is critical for genomic stability. However, mechanisms that limit the access of low-fidelity DNA polymerases, such as polymerase η (Pol η), to the replication fork are not well understood or characterized. Both classes of polymerases share a common mechanism to access the DNA primer/template (P/T) terminus by the possession of a PCNA-interacting peptide (PIP) motif (Choe and Moldovan, 2017).

Upon exposure to stresses that cause DNA lesions, maintenance of the integrity of the replication fork becomes a major priority (Segurado and Tercero, 2009). Replicative polymerases are blocked by bulky lesions on the template strand, leading to stalling of the replication fork. Failure to resolve the stalled fork in a timely manner leads to fork collapse and likely cell death (Cortez, 2015; Roos and Kaina, 2006). Under these circumstances, the DNA damage tolerance pathway is activated, leading to the recruitment of translesion synthesis (TLS) Pols (Goodman and Woodgate, 2013; Waters et al., 2009). These Pols displace replicative polymerases at the lesion sites to replicate across the lesion and rescue the stalled fork. Pol η is the most intensively studied of TLS Pols, and it replicates across UV-induced lesions, especially cyclobutane pyrimidine dimers (CPDs) formed between neighboring pyrimidine bases in DNA, with high accuracy (Johnson et al., 1999; Masutani et al., 2000). It is not essential for routine DNA replication and Pol η-null mice display normal size, fertility, and life expectancy in the absence of external DNA damage (Lin et al., 2006). However, germline loss of Pol η function results in increased UV sensitivity and propensity for cancer in a subset of patients with xeroderma pigmentosum (XP) (Cordonnier and Fuchs, 1999), the variant form (XP-V).

The ability of Pol η to replicate across bulky lesions arises from a relatively more spacious active site (Silverstein et al., 2010; Zhao et al., 2012) when compared with those of Pol δ and Pol ε. However, this property also contributes to its reduced replication fidelity (Kunkel, 2003). Pol η is about 10,000 times (error rate of ~1/100) more error-prone than Pol δ or Pol ε when replicating normal templates, typified by the signature mutations of A to G or C to T transitions under certain sequence contexts (Chen and Sugiyama, 2017; Matsuda et al., 2001). Both types of mutations have been observed in a number of recently identified cancer mutational signatures (Rogozin et al., 2018; Rubin and Green, 2009; Supek and Lehner, 2017). Thus, it is

[1]Department of Biochemistry and Molecular Biology, New York Medical College, Valhalla, NY 10595, USA

[2]Department of Pathology, New York Medical College, Valhalla, NY 10595, USA

[3]Present address: ADDL-Purdue University, 406 S. University, West Lafayette, IN 47907, USA

[4]Lead Contact

*Correspondence: zhongtao_zhang@nymc.edu

https://doi.org/10.1016/j.isci.2018.07.009

prohibitive for unregulated participation of Pol η in routine DNA replication, a process that demands an error rate of less than one in a billion.

The mechanisms that regulate the recruitment of Pol η to DNA damage sites initially seemed to be clearly defined. It was discovered that monoubiquitination on K164 of PCNA (Ub-PCNA) by RAD6/RAD18 is critical for UV resistance in *Saccharomyces cerevisiae* (Hoege et al., 2002). Two subsequent studies demonstrated that yeast Pol η activity is stimulated by Ub-PCNA through its possession of a ubiquitin-binding domain (UBZ) in its non-catalytic C-terminal sequence (Garg and Burgers, 2005; Watanabe et al., 2004). These studies painted a clear picture of recruitment and regulation: monoubiquitination of PCNA induced by DNA damage stress recruits Pol η through enhanced affinity to the damage site to perform TLS (Kannouche et al., 2004). However, *in vitro* reconstitution studies (Acharya et al., 2007, 2008; Bertoletti et al., 2017; Jung et al., 2011; Ma et al., 2017; Sabbioneda et al., 2009) provided contradicting results and failed to recapture the elegance of the proposed model (Hedglin et al., 2016). Furthermore, subsequent cellular studies failed to resolve the ambiguities (Acharya et al., 2010; Kannouche et al., 2001).

Meantime, accumulating evidence suggests that post-translational modifications (Chen et al., 2008; Dai et al., 2016; Göhler et al., 2011; Jung et al., 2011) of Pol η and interactions with partner proteins play major roles in its regulation (Maga et al., 2013; Tissier et al., 2010). Among these, two studies demonstrated that phosphorylation of Pol η by *ataxia telangiectasia* and Rad3 related (ATR) (Göhler et al., 2011) and protein kinase C (PKC) (Chen et al., 2008) is critical for its function in intact cells.

We aimed to resolve some of the aforementioned inconsistencies through comparative studies on wild-type (WT) and phosphomimetic mutants (PM) of Pol η. Our data show that phosphorylation of Pol η greatly potentiates its activity when Ub-PCNA is present, which reveals a mechanism whereby phosphorylation of Pol η enhances its affinity for Ub-PCNA. This mechanism sheds new light not only on the control of TLS but also on the avoidance of Pol η participation in normal DNA replication.

On the protein interaction front, PDIP38 proved to be an intriguing partner. PDIP38 interacts with the C-terminal UBZ domain (Tissier et al., 2010) of Pol η and was proposed to facilitate the recruitment of Pol η to UV-induced DNA damage sites. In *in vitro* reconstitution studies, PDIP38 stimulated the activities of Pol η (Maga et al., 2013). However, there has been no evidence showing that PDIP38 localizes to DNA damage foci with TLS Pols. In fact, PDIP38 is translocated to the spliceosome upon UV exposure (Wong et al., 2013). Our studies show that PDIP38 acts as a key regulator in restricting Pol η participation in DNA replication in unstressed cells.

RESULTS

Phosphorylation Activates Pol η

To address the effects of ubiquitination of PCNA and phosphorylation on Pol η activities, we performed *in vitro* experiments using recombinant Pol η. Human Pol η possesses a UBZ domain that readily unfolds when stripped of a required zinc ion by EDTA (Woodruff et al., 2010); thus variable loss of UBZ function could give rise to a range of variations in Pol η properties. We took specific steps to maintain the functional integrity of its UBZ domains. We generated recombinant Pol η tagged at the C-terminus with six histidine residues by overexpression in *E. coli* strain Rosetta 2 (DE3). The expression level and solubility were further optimized by co-expression with ubiquitin, which can interact with the UBZ domain and stabilize Pol η. Zinc-charged chelating resin was used for purification of Pol η, instead of the traditionally used Ni-charged resins, to avoid metal ion exchange and maintain proper UBZ folding. Detailed protocols are provided in Supplemental Information. All recombinant Pol η preparations were over 90% pure and monomeric upon characterization by gel filtration chromatography (Figure S1). A phosphomimetic mutant of Pol η was also expressed to investigate the effects of phosphorylation on its activity. This phosphomimetic mutant (Pol η^{PM}) bears glutamate residues at the aforementioned phosphorylation sites for PKC (S587, T617) (Chen et al., 2008) and ATR (S601) (Göhler et al., 2011).

To validate our enzyme production and purification procedure, we conducted single nucleotide incorporation assays using protocols adopted from reports in the literature (Guilliam et al., 2016; Maga et al., 2013; Washington et al., 2003). Steady-state kinetic analysis indicates that Pol η exhibits similar catalytic constants in terms of K_m (0.15 μM for dATP opposite of dTTP) as reported in the literature, and the k_{cat} value (0.22 s^{-1}) is similar to that reported by Washington et al. (2003).

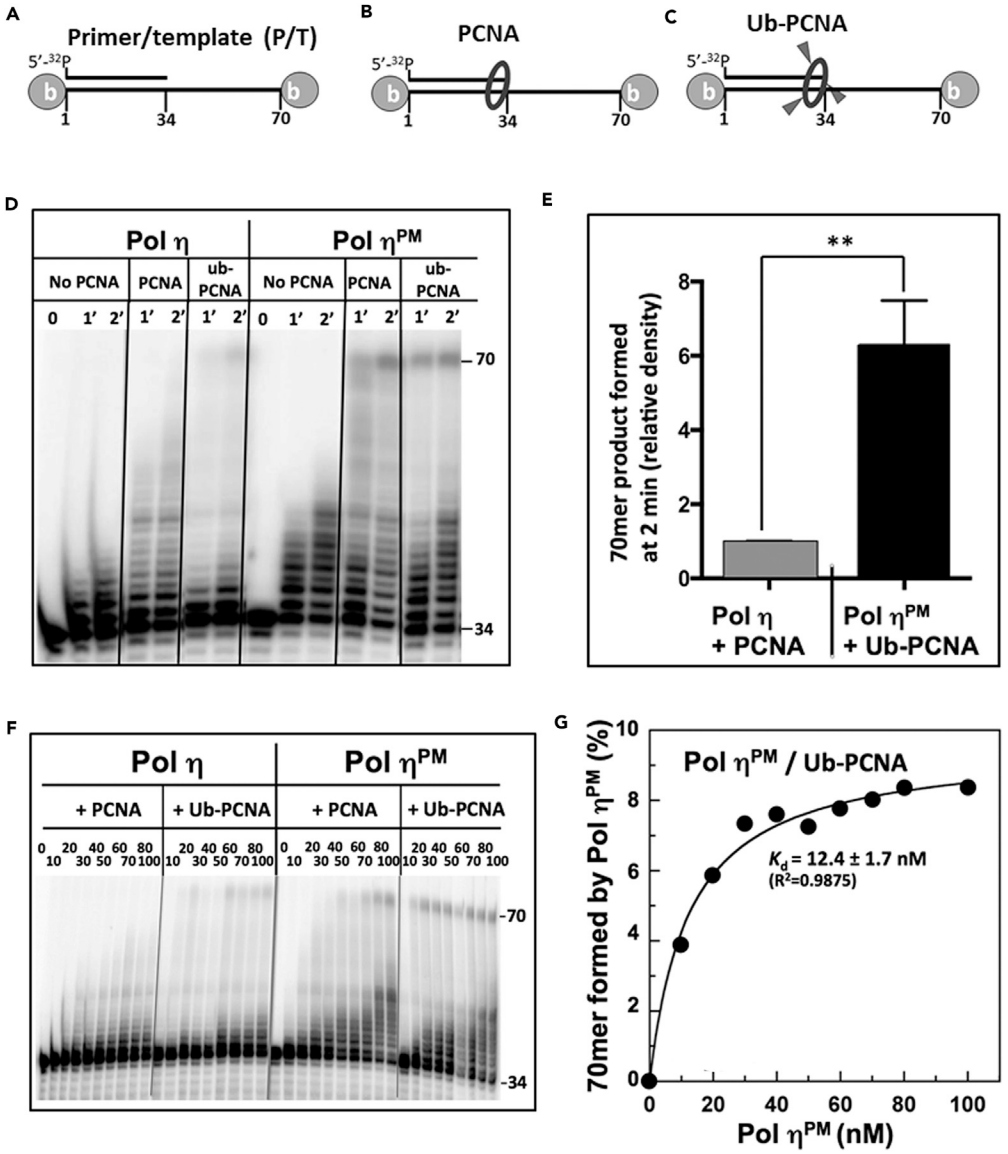

Figure 1. Phosphomimetic Pol η Exhibits Increased Activity

(A–C) (A) Schematic representation of ^{32}P-labeled primer/template (P/T). P/T pre-loaded with PCNA (B) or Ub-PCNA (C). The template was modified by biotinylation on both ends and blocked with streptavidin.

(D) Representative sequencing gel showing resolved extension products at 1 and 2 min. The labeled primer and the full-length product are indicated as 34 and 70, respectively.

(E) Relative quantification of full-length 70mer products of Pol η^{PM} with Ub-PCNA normalized to Pol η with PCNA at 2 min. Data shown as mean ± SD of 3 individual experiments and differences between groups analyzed by unpaired t test, $^{**}p \leq 0.01$.

(F and G) Extension products of increasing concentrations of Pol η or Pol η^{PM} (10–100 nM) titrated against a fixed concentration of either PCNA-loaded P/T (+PCNA) or Ub-PCNA-loaded P/T (+Ub-PCNA) at 2 min. The 70mer extension products formed by Pol η^{PM} on Ub-PCNA-loaded P/T in (F) were analyzed and fitted to one-site binding kinetics (G).

Upon validation of our purified enzymes, we sought to investigate the role of Pol η in two cellular processes: routine DNA replication and TLS. Pol η replicates native and CPD-lesioned templates with similar efficacy (Johnson et al., 2005; Masutani et al., 2000; Yagi et al., 2005), with the determining factor being the efficacy with which Pol η binds to the P/T terminus. Therefore, a single pair of primer and template without lesions was used in both assays for fair comparison. The substrate consisted of a 70mer template with a 34mer primer radiolabeled at the 5′ end by ^{32}P (Figure 1A). The template was modified at both ends with biotin

and blocked with streptavidin to allow quantitative pre-loading of PCNA (Figure 1B) or Ub-PCNA (Figure 1C) by human replication factor C (RFC) (Lin et al., 2013). Concentrations of RFC were chosen such that P/T > RFC > PCNA or Ub-PCNA to favor the complete loading of PCNA and Ub-PCNA to the P/T termini. Assay conditions were chosen to mimic the cellular ionic environment in terms of pH, ion type, and strength. Specifically, the assay buffer contained 150 mM KCl and 50 mM NaCl (the ionic environment of nuclei consists of 150–260 mM KCl and 40 to 50 mM NaCl [Dick, 1978; Paine et al., 1981]).

The primer extension activities of Pol η and Pol η^{PM} in the absence or presence of either pre-loaded PCNA (Figure 1B) or pre-loaded Ub-PCNA (Figure 1C) were compared. The reactions were initiated by the addition of Pol η and terminated at 1 and 2 min. A representative autoradiogram of the primer extension products is shown in Figure 1D. The activities of both Pol η and Pol η^{PM} are stimulated by PCNA, and even more so by Ub-PCNA (Figure 1D). The results are consistent with the models in which the PIP-motifs in Pol η are functionally effective in stimulating Pol η activity in the presence of PCNA, and causing a greater increase in Pol η activity (Figure 1D, first 3 lanes) with the binding of the added ubiquitin on Ub-PCNA. However, Pol η^{PM} is much more active than Pol η, as can be seen by the production of the full-length products (70mer) (Figure 1D, last 3 lanes). These findings show for the first time that phosphorylation of Pol η is a mechanism that leads to a significant activation of Pol η. This is illustrated by comparison of the activity of Pol η on a PCNA-loaded P/T and Pol η^{PM} on an Ub-PCNA loaded P/T (Figure 1E). The Pol η^{PM}/Ub-PCNA combination forms ~7× more 70mer products than the Pol η/PCNA.

To investigate the mechanisms leading to the activation of Pol η, a series of titration studies were performed in which the concentrations of Pol η or Pol η^{PM} were increased from 10 to 100 nM, whereas the substrate concentrations were kept constant (Figure 1F). A similar pattern of activity changes as found in the previous assay (Figure 1D) was observed. Pol η was more active with Ub-PCNA than PCNA, and in both cases, Pol η^{PM} was much more active than Pol η. A plot of 70mer product formation against Pol η^{PM} for substrate P/T/Ub-PCNA showed that Pol η^{PM} exhibits one-site binding kinetics with an apparent K_d of 12.4 ± 1.7 nM (Figure 1G). Analysis for Pol η/Ub-PCNA or Pol η^{PM}/PCNA combinations indicated that the plots did not reach the saturation part of the curve (indicating K_d values of greater than 100 nM, Figure S1). Taken together, the above-mentioned observations indicate that optimal DNA TLS by Pol η requires phosphorylation of the enzyme as well as monoubiquitination of PCNA.

Phosphomimetic Pol η Binds Tightly to Ub-PCNA

The titration studies presented above demonstrated that Pol η^{PM} has an enhanced affinity for Ub-PCNA pre-loaded onto a P/T terminus. This affinity could reflect the affinity of Pol η^{PM} for either Ub-PCNA per se or the P/T/Ub-PCNA complex. To distinguish between these possibilities, we directly assessed the association of Pol η^{PM} with Ub-PCNA in the absence of DNA. Various size exclusion chromatographic techniques are commonly used to characterize both dynamic and stable protein-protein interactions (Bai, 2015; Beeckmans, 1999). The PIP box-PCNA interactions are examples of the dynamic interactions that facilitate Okazaki fragment maturation process (Choe and Moldovan, 2017; Lin et al., 2013). Thus, a majority of PCNA interactions are transient in nature, with the affinities (K_d) between PIP boxes and PCNA ranging from 10^{-4} M to 10^{-7} M (Bruning and Shamoo, 2004; Pedley et al., 2014). On the other hand, subunits of a holoenzyme generally form stable complexes with dissociation half-lives of hours or longer, and dissociation rates are difficult to measure by quantitative methods. The classical size-exclusion technique is suited for the analysis of these stable complexes. Fast protein liquid chromatography gel filtration (Supplemental Information) was used to investigate the strength of interaction between Pol η^{PM} and Ub-PCNA. High-ionic-strength buffers (350 mM NaCl) were used to eliminate any potential non-specific interactions.

Upon establishing individual elution profiles of Pol η^{PM} and Ub-PCNA (Figures 2A–2D), we mixed Pol η^{PM} with Ub-PCNA in a molar ratio of 1:2 (6 μM and 12 μM, calculated as Ub-PCNA trimer, in a total volume of 100 μL) and applied the mixture to a Superdex 200 10/300 GL column (GE). The elution profiles as well as SDS-PAGE analysis (Figures 2E and 2F) revealed that Pol η^{PM} and Ub-PCNA formed a stable complex in a 1:1 molar ratio. Incidentally, the SDS gel for the column fractions (Figure 2F) demonstrated that practically all of the Pol η^{PM} is engaged in complex formation, confirming the integrity of the preparation with regard to the functionality of UBZ domains. The absolute requirement for an intact UBZ domain for this binding was demonstrated by the inclusion of EDTA (Figures S2A and S2B), which acts to remove the zinc required for the folding of UBZ domain (Woodruff et al., 2010). The disruption of ubiquitin-Pol η^{PM} interaction by EDTA was further demonstrated by pull-down assays with glutathione S-transferase (GST)-ubiquitin (Figures S2C and S2D).

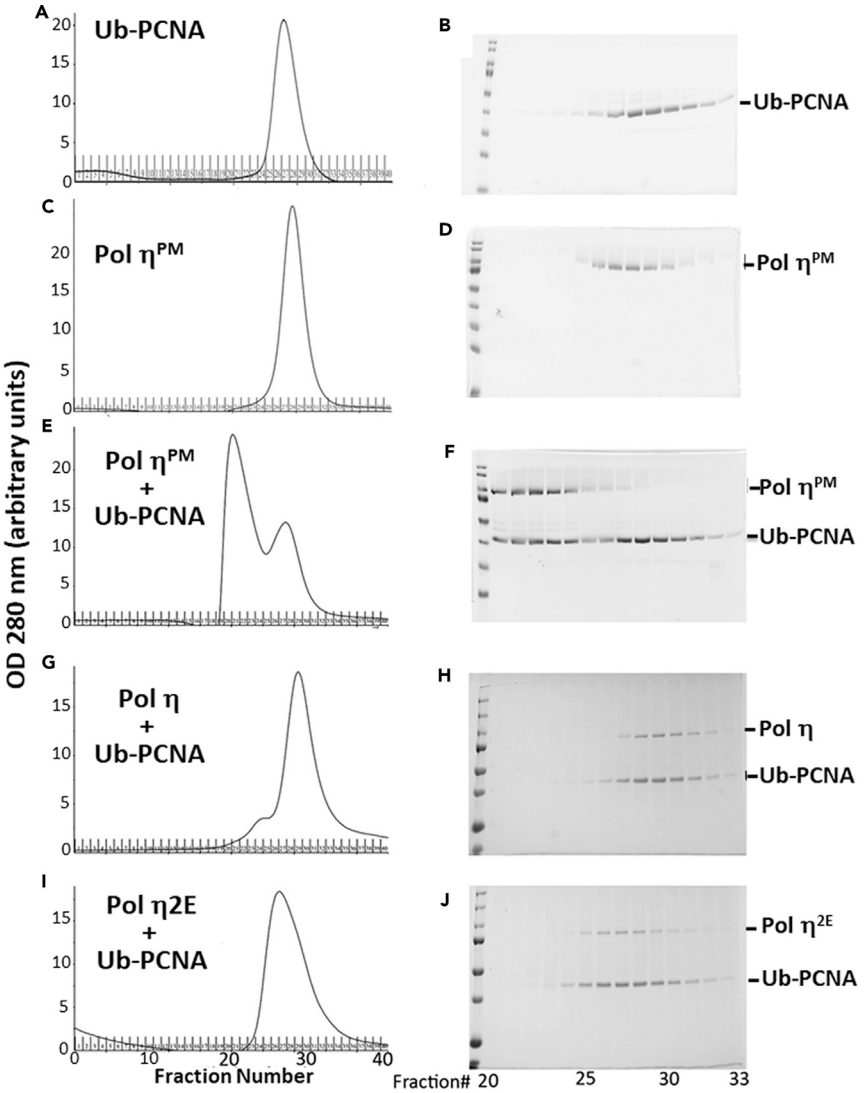

Figure 2. Pol η^{PM} and Monoubiquitinated PCNA form a High-Affinity Complex

Elution profiles of Superdex 200 10/300 GL column are shown on the left, and the corresponding fractions analyzed by SDS-PAGE analysis and Coomassie blue staining are shown on the right.

(A–J) (A and B) Ub-PCNA, (C and D) Pol η^{PM}, (E and F) Pol η^{PM} and Ub-PCNA mixture, (G and H) Pol η and Ub-PCNA mixture, and (I and J) phosphomimetic mutant Pol η^{2E} (S601E and T617E) and Ub-PCNA mixture.

These interactions depend on the phosphomimetic mutation of Pol η on the aforementioned ATR and PKC sites. Neither the WT enzyme nor a Pol η mutant (Pol η^{2E}) with two of the residues mutated to glutamates (S587E and S601E) formed a tight complex with Ub-PCNA when assayed under identical conditions (Figures 2G–2J). However, the Pol η^{2E} mutant shows a slight shift on gel filtration (Figure 2J) and may indicate enhanced yet dynamic interaction with Ub-PCNA. These studies demonstrate that Pol η^{PM} and Ub-PCNA form a complex in a 1:1 molar ratio with affinities reminiscent of those between subunits of holoenzymes, which have a dissociative half-life of hours or longer (Bai, 2015; Beeckmans, 1999).

Phosphorylated Pol η at the Primer/Template/Ub-PCNA Terminus Cannot be Readily Displaced by Pol δ

The preceding experiments show that Pol η^{PM} binds to Ub-PCNA with high affinity. Under physiological conditions, the binding of phosphorylated Pol η would occur in the presence of Pol δ as a competitor. To investigate the possible exchange of Pol η with Pol δ, we constructed a synthetic P/T with Ub-PCNA

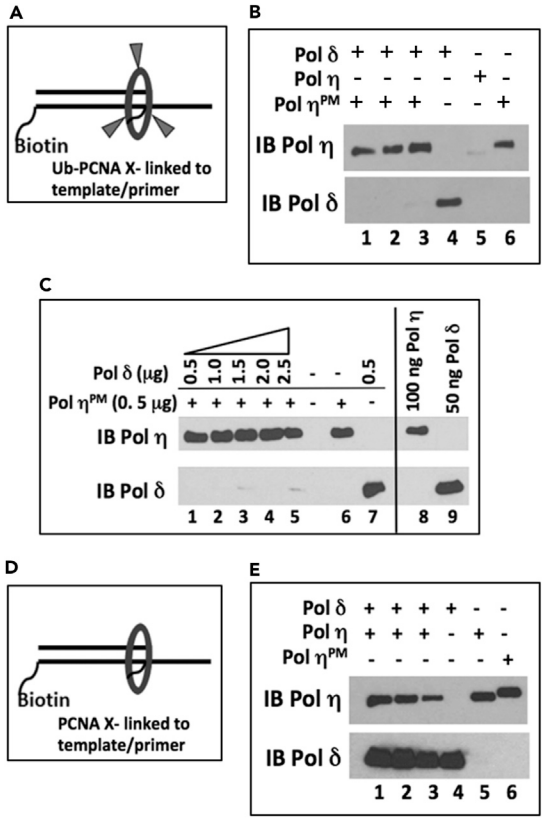

Figure 3. Pol η^{PM} on P/T/Ub-PCNA Terminus Is Resistant to Displacement by Pol δ

(A) Schematic representation of Ub-PCNA cross-linked to a primer/template (P/T).

(B) Lanes 1–3 (triplicates) contain 0.5 μg each of Pol δ and Pol η incubated with ~100 ng binding capacity of Ub-PCNA-loaded P/T beads for 2 hr at 4°C. The beads were then washed with a stringent protocol. Lanes 4–6 are control reactions with 0.5 μg of individual proteins incubated with Ub-PCNA-loaded P/T beads. Bound proteins were detected by western blotting with antibodies against Pol η and Pol δ (p68 subunit).

(C) Increasing amounts of Pol δ (0.5–2.5 μg) incubated with 0.5 μg of Pol η^{PM} (lanes 1–5). Lanes 6 and 7 are control lanes with each protein individually. Lanes 8 and 9 are input.

(D) Schematic representation of PCNA cross-linked to a P/T.

(E) Binding of a mixture of Pol δ and Pol η to P/T/PCNA beads was performed as in (B). The beads were washed 3× with PBS, and bound proteins detected by western blot.

(or PCNA) covalently linked near the primer terminus by N-hydroxysuccinimide(NHS)-psoralen (Figures 3A and 3D; Supplemental Information and S3). The complex was immobilized to streptavidin beads through the biotin-modified template at the 5′ end. We titrated the binding capacity of both beads: P/T/Ub-PCNA beads bind Pol η (60–90 ng/μL) and Pol δ (170–200 ng/μL). The P/T/PCNA beads bound about 2.5× greater amounts of these proteins than the /P/T/Ub-PCNA beads.

The initial experiments utilized P/T/Ub-PCNA beads to mimic a stalled replication fork post-UV irradiation. A limiting amount of P/T/Ub-PCNA beads (1 μL, <100 ng capacity) was used to bind a mixture of Pol η^{PM} (500 ng) and Pol δ (500 ng) in addition to control samples where individual proteins were used (Figure 3B). The binding buffer contained 160 mM KCl and 50 mM NaCl to maintain ionic strength comparable to that of nucleus (25 mM HEPES, pH 7.5). In addition, zinc (5 μM) and citrate (10 mM) were added to maintain a constant zinc ion concentration. The zinc-citrate complex has an apparent dissociation constant of 1.17×10^{-12} M^2 (Krezel and Maret, 2016), and therefore our additions produce conditions close to cellular soluble zinc ion concentrations (Krezel and Maret, 2006). After incubation at 4°C for 2 hr, unbound proteins were washed by binding buffer with a stringent washing protocol (5×, 10-min incubation each). Bound proteins were analyzed by western blot analysis to detect Pol η and Pol δ (p68 subunit). Regardless of the presence (Figure, 3B, lanes 1–3, triplicates) or absence (lane 6) of Pol δ, Pol η^{PM} bound to full capacity

of the beads, whereas Pol δ could not be detected when Pol η^{PM} was present (lanes 1 to 3). Under identical conditions, Pol η alone showed minimal binding (Figure 3B, lane 5) and Pol δ alone bound to 20%–30% of beads capacity (Figure 3B, lane 4). To characterize the interactions further, we increased the concentration of Pol δ while keeping the concentration of Pol η^{PM} constant (Figure 3C). Regardless of how high the Pol δ concentration was, Pol η^{PM} still bound to the full capacity of the beads, whereas no detectible Pol δ was bound (Figure 3C, lanes 1–5). These observations indicate that ATR- and PKC-phosphorylated Pol η will bind P/T/Ub-PCNA terminus regardless of the presence of related replicative Pols.

The binding preference of P/T/PCNA beads (Figure 3D) was also examined with a milder wash method, as the stringent washing protocol reduced the signal beyond detection. The aim of these experiments was to evaluate the extent to which Pol η can interfere with routine DNA replication process by Pol δ. Under milder washing conditions, Pol δ bound to DNA to a similar extent in the presence (Figure 3E, lanes 1–3, triplicates) or absence of Pol η (lane 4). Pol η also displayed similar binding to P/T/PCNA in the presence (Figure 3E, lanes 1–3) or absence of Pol δ (lane 5). In essence, bindings of Pol δ or Pol η to P/T/PCNA terminus are dynamic processes, which is consistent with studies of polymerase transactions on PCNA (Hedglin et al., 2016). These data do pose an important question: how is Pol η kept away from participation in routine DNA replication process under cellular conditions? Our *in vitro* assays mentioned above have shown that replication termini loaded with PCNA apparently recruited Pol δ and Pol η with similar efficacies in the absence of DNA damage stress. There must be additional mechanisms that prevent Pol η from participating in routine DNA replication.

Phosphorylation Is Responsible for Pol η Persistence at the Damage Foci

Having demonstrated that Pol η^{PM} and Ub-PCNA form a tight complex, which does not readily dissociate, we sought to replicate these findings under cellular conditions. We attempted to generate stable cell lines with ectopic expression of GFP-Pol η^{PM} as well as WT and a phosphorylation-deficient mutant (all three residues to A, Pol η^{3A}). Cells expressing the WT enzyme were stable as established in many laboratories (Bienko et al., 2010; Kannouche et al., 2001; Watanabe et al., 2004), as were Pol η^{3A}-expressing cells. However, repeated attempts to establish a stable GFP-Pol η^{PM} expression cell line failed. We tried immortalized XPV cells (GM02359-hTERT and XP30RO), 293T cells, and MRC5 lung cells with either antibiotic selection or lentiviral infection. Initially, all three constructs were transfected with similar efficiency judging by the fluorescence signals. However, cells expressing Pol η^{PM} gradually died and no cells with fluorescent signals survived after 2 weeks. Thus, the overexpression of Pol η^{PM} is clearly toxic to the cells. Therefore, we compared the fluorescent signal and localization of Pol η and Pol η^{PM} on a transient transfection basis within 48 hr in both 293T and MRC5 cells. Examination under the microscope at 36 hr after transfection revealed that ectopic expression of GFP-Pol η^{PM} resulted in the formation of bright foci. Even though WT Pol η has been shown to form some relatively large foci, the Pol η^{PM} foci are more intense with sharper boundaries and are significantly more in number (Figures 4A and 4B, MRC5 cells). We analyzed approximately 60 GFP cells in a single continuous field. Pol η^{PM} -expressing cells formed 4 times as many foci per cell (52.5) as Pol η-expressing cells (13.7), and with more cells (56.5% versus 21.7%) with 20 or more foci.

Upon UV-C irradiation (30 J/m^2), Pol η (Figure 4C) as well as Pol η^{PM} (Figure 4D) formed bright foci after fixation with formalin. Even Pol η^{3A} showed some diffused foci (Figure 4E). Our *in vitro* studies with Pol η^{PM} suggest that the binding of phosphorylated Pol η to Ub-PCNA at the damage sites on chromatin would no longer be a dynamic process, i.e., phosphorylated Pol η-Ub-PCNA or Pol η^{PM}-Ub-PCNA foci will have limited dynamic exchange with non-chromatin bound Pol η. However, technical proof of this phenomenon is complicated by the fact that Pol η/PCNA foci could arise from many combinations. Phosphorylated Pol η (or Pol η^{PM}) also possess tendencies to be recruited by PCNA (as shown without UV stress, Figure 4B). In addition, Ub-PCNA can also recruit Pol η to a greater extent than PCNA regardless of the phosphorylation status (Figure 1D). Indeed, earlier studies using fluorescence quenching methods showed that there are mixed populations of Pol η at the foci as well (Sabbioneda et al., 2008).

We took a different approach to investigate the stability of the Pol η^{PM} and Ub-PCNA complex. We perforated the cytoplasmic and nuclear membranes with buffers containing 1% Triton X-100 (Kannouche et al., 2001) and high salt concentrations (150 mM KCl and 50 mM NaCl) before fixation with formalin. We hypothesized that proteins not bound to chromatin or bound to chromatin dynamically would be washed away at room temperature with excess buffer; hence only proteins stably bound to chromatin would be observed. Upon perforation, transfected cells were washed extensively at room temperature with shaking for 5 to

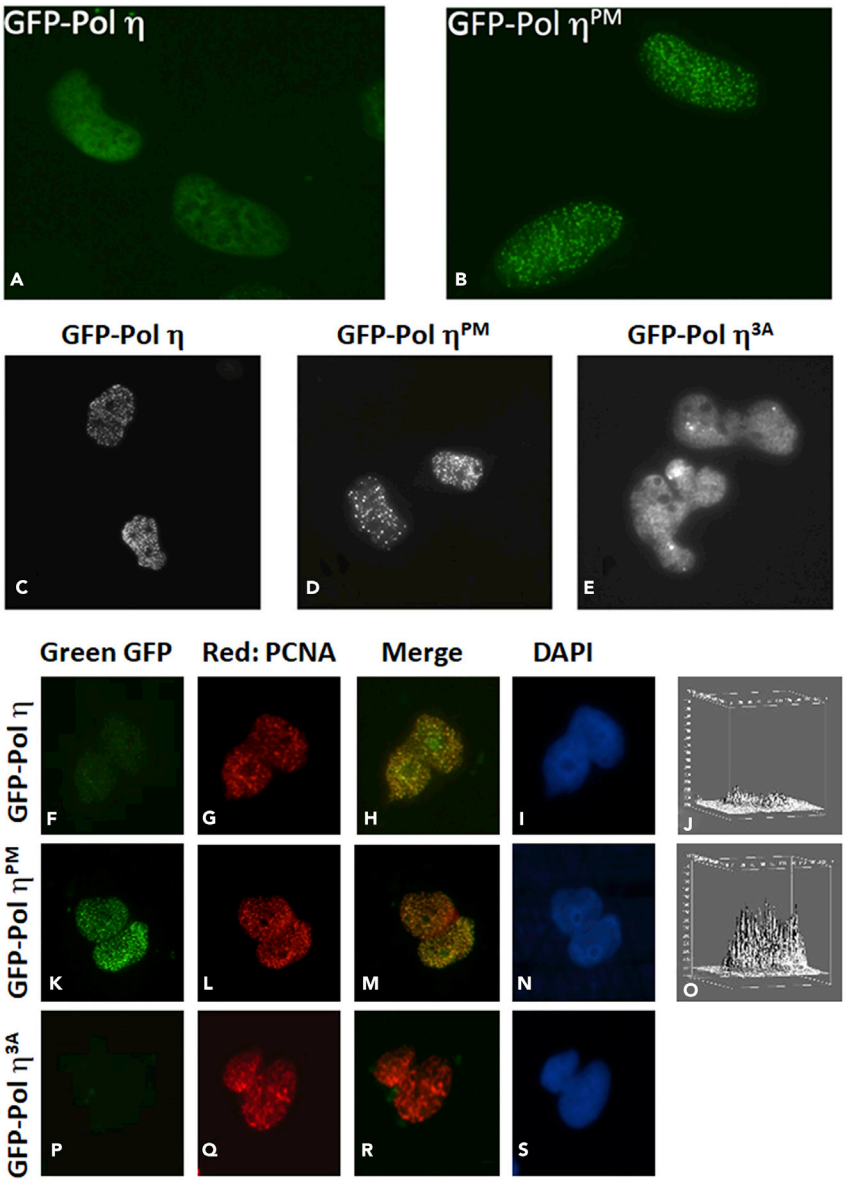

Figure 4. Efficient Retention of Pol η on UV-Induced DNA Damage Foci Requires Phosphorylation

(A and B) MRC5-SV2 cells were transfected with GFP- Pol η (A) or GFP- Pol η^{PM} (B) and fixed with 4% paraformaldehyde 36 hr later and imaged at 66X.

(C–E) MRC5-SV2 cells were transfected with GFP- Pol η, GFP-Pol η^{PM}, or GFP- Pol η^{3A} and 36 hr later exposed to 30 J/m^2 of UV-C. Cells were allowed to recover for 5 hr before subsequent fixation by 4% paraformaldehyde and imaged.

(F–S) 293T cells transfected with the GFP-Pol η (F–J), GFP- Pol η^{PM} (K–O), and GFP- Pol η^{3A} (P–S) were exposed to UV irradiation 36 hr later. After recovery for 5 hr, cells were extracted with 1%Triton X-100-containing buffer at room temperature (~22°C) before fixation by methanol at −20°C. Subsequently cells were imaged at 66× magnification. GFP signal exposures were maintained constant across samples. The strength of individual foci fluorescence for panels F and K were mapped using the 3D surface plot plug-in of ImageJ (J and O). Merge indicates the stacking of the GFP (green) and the PCNA (red) fluorescence signals, GFP intensity adjusted to indicate localization.

8 min. The effectiveness of the washing protocol is illustrated by the total disappearance of fluorescence signal from the nuclei of GFP-Pol η^{3A} cells (Figure 4P). In either 293T or MRC5 cells, this wash protocol has minimal impact on the number of foci in cells expressing WT Pol η or Pol η^{PM} (Figures 4F and 4K). Some loss of fluorescence intensity, especially in WT-Pol η-expressing cells (Figure 4F, all figures are adjusted for equal exposure) was observed. The individual foci were mapped for Pol η and Pol η^{PM} green

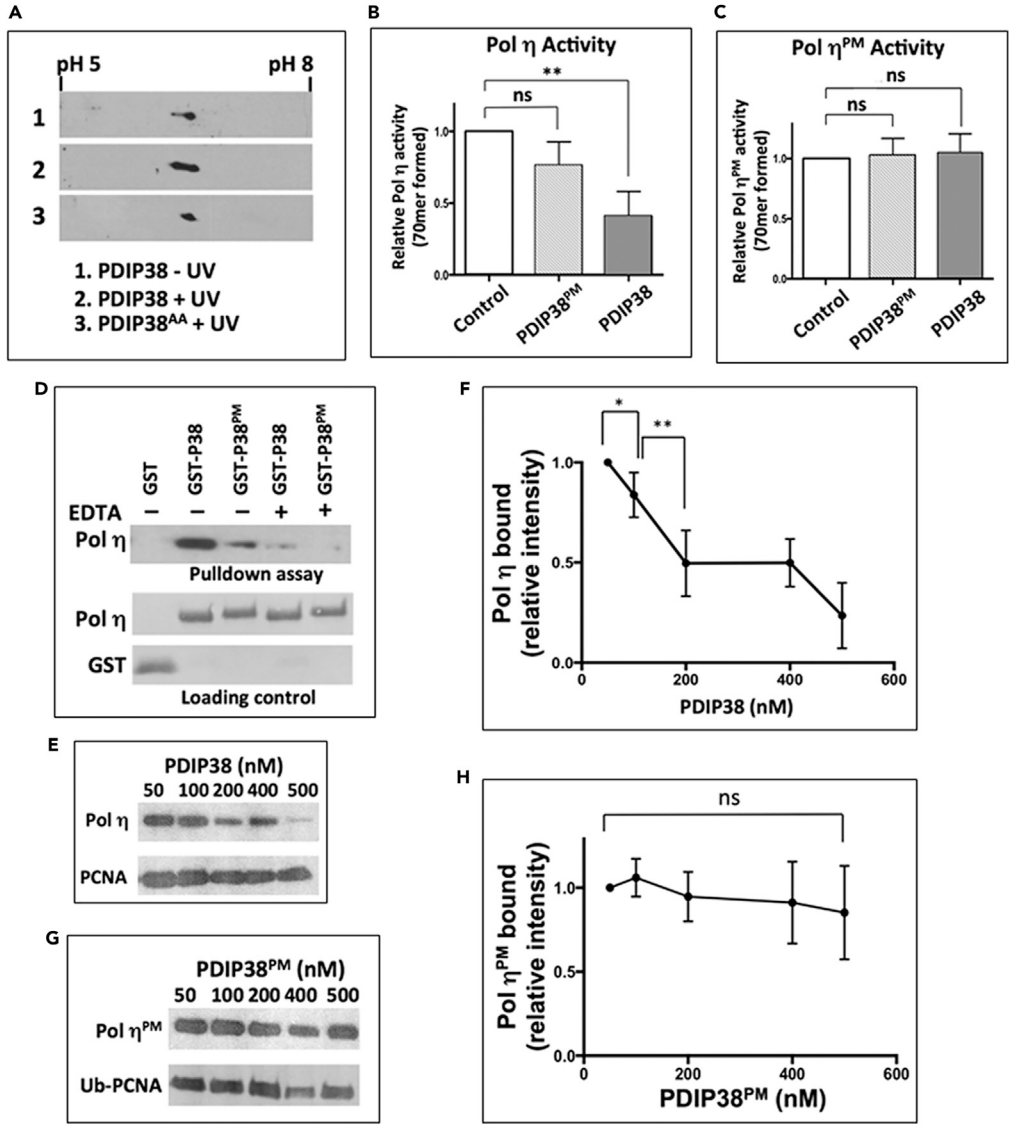

Figure 5. PDIP38 Sequesters Pol η from Normal Replication Fork

(A) 2D gel electrophoresis of nuclear extract of 293T cells transfected with Flag-tagged PDIP38 (full-length with C-terminal tag) and its phosphorylation-deficient mutant, PDIP38^{AA}. 24 Hours after transfection, cells were exposed to 30 J/m^2 of UV-C irradiation and allowed to recover for 5 hr. Nuclear fractions were prepared and subsequently resolved by 2D gel electrophoresis before being transferred to nitrocellulose. PDIP38 was identified by anti-Flag antibody. The pH range (5–8) of the isoelectric focusing strip range is indicated above.

(B) Effects of PDIP38 (200 nM) on Pol η activity in primer extension assays using P/T/PCNA (see Figure 1B). The extension products were analyzed on sequencing gel and quantified (70mer product, 2 min) (Figure S5A). Data shown as mean ± SD of 3 individual experiments, and differences between groups analyzed by unpaired t test. **$p < 0.01$.

(C) Effects of PDIP38^{PM} (200 nM) on Pol η^{PM} in primer extension assays using P/T/Ub-PCNA (see Figure 1C). A representative extension gel is included in Figure S5B. The extension products were analyzed on sequencing gel and quantified (70mer product, 2 min). Data shown as mean ± SD of 3 individual experiments and differences between groups analyzed by unpaired t test. ns indicates not significantly different.

(D) Pull down of recombinant Pol η using GST-tagged PDIP38 and its phosphomimetic mutant, PDIP38^{PM}. Pol η (500 ng) was pulled down with GST, GST-PDIP38, or GST-PDIP38^{PM}. To demonstrate the requirement for an intact UBZ domain, the pull-down assays were performed in the presence of 2 mM EDTA. Ponceau staining of GST-tagged proteins as loading controls is shown. Pol η bound to beads was analyzed by western blot.

(E and F) Effects of PDIP38 on binding of Pol η to P/T/PCNA beads. Each condition had 0.5 μg Pol η incubated with 100 ng binding capacity of PCNA-loaded P/T beads in the presence of increasing concentration of PDIP38 (50 nM–500 nM) for 2 hr at 4°C. After subsequent washes with PBS, the beads were boiled and bound proteins detected by western blot

Figure 5. *Continued*

against Pol η to detect the amount bound to PCNA cross-linked P/T. PCNA was also detected as a loading control. Data shown as mean ± SD of 3 individual experiments, and differences between groups analyzed by unpaired t test, $^{**}p < 0.01$, $^{*}p < 0.05$.

(G and H) Effects of PDIP38^{PM} on binding of Pol η^{PM} to P/T/Ub-PCNA beads. Each condition had 0.5 μg Pol η^{PM} incubated with 100 ng binding capacity of Ub-PCNA-loaded P/T beads in the presence of increasing concentration of PDIP38^{PM} (50–500 nM) for 2 hr at 4°C. After subsequent washes with PBS, the beads were boiled and bound proteins detected by western blot against Pol η to detect the amount bound to Ub-PCNA cross-linked P/T. Ub-PCNA was also detected as a loading control by using antibody against PCNA. Data shown as mean ± SD of 3 individual experiments, and differences between groups analyzed by unpaired t test, ns indicates not significantly different. Statistical comparison between presence of 50 nM PDIP38^{PM} and 500 nM PDIP38^{PM} is indicated.

fluorescence with ImageJ (Figures 4J and 4O). The fluorescence signals from the foci of the whole-cell populations were further quantified by laser scanning cytometry (Figure S4). Taken together, these data suggest that transfected Pol η^{PM} is recruited to the replication fork by PCNA-loaded primer ends even in the absence of UV stress, which could account for observed cell death. Post UV exposure, phosphorylated Pol η binds to Ub-PCNA and forms a stable complex that does not readily dissociate.

PDIP38 Sequesters Pol η from Participation in Routine DNA Replication in Unstressed Cells

The preceding studies show the importance of excluding Pol η from DNA replication except when absolutely needed. The mechanism(s) that exclude Pol η from the DNA are not fully understood. One likely mechanism is the association of Pol η with PDID38, based on previous observations that PDIP38 binds Pol η (Maga et al., 2013; Tissier et al., 2010). However, PDIP38 is subsequently enriched in the spliceosomes instead of the DNA repair foci in response to UV stress (Wong et al., 2013). Therefore, we hypothesize that PDIP38 sequesters Pol η away from replication fork to prevent its participation in DNA replication in unstressed cells.

Our laboratory has observed that PDIP38 is phosphorylated post-UV irradiation (Figure S5) in an ATR-dependent manner. PDIP38 possesses two potential ATR phosphorylation sites at Ser147 and Ser150. Ectopic expression of Flag-tagged Wt PDIP38 and its phosphorylation-null mutant, PDIP38^{AA} (S147A/S150A), followed by 2D gel electrophoresis (Figure 5A) showed that these two residues are targeted for UV-induced phosphorylation.

In the next set of experiments, we investigated the impact of direct PDIP38-Pol η interaction on the enzymatic activities in conditions mimicking pre- and post-UV irradiation. To conduct reconstitution studies, we optimized the production of the recombinant PDIP38. Using standard protocols, PDIP38 expressed in *E. coli* does not fold well and is present mainly as insoluble inclusion bodies (Maga et al., 2013). PDIP38 purified from the soluble fraction did not behave consistently in our hands. Therefore, we optimized the expression system and discovered that osmotic stress (0.5 M NaCl and 1 mM betaine) (Oganesyan et al., 2007) provided the optimal conditions. Under these conditions, the recombinant PDIP38 was soluble and exhibited minimal degradation (Figure S1B). We purified PDIP38 and its phosphomimetic mutant, as well as the GST fusion variants of these proteins (Figure S1B). The phosphomimetic mutant (PDIP38^{PM}) was constructed by mutation of serine 147 and 150 to glutamates within the ATR consensus sequence (Kim et al., 1999) SQRSQ.

The effects of PDIP38 and PDIP38^{PM} on Pol η and Pol η^{PM} activities were examined using the P/T substrates loaded with PCNA or Ub-PCNA (see Figures 1B and 1C). Representative gels are shown in Figures S6A and S6B. When PCNA loaded P/T was used in the activity assays, which represented routine DNA replication, PDIP38 inhibited Pol η activity (Figure 5B), whereas PDIP38^{PM} did not show any significant inhibition (Figure 5B). When Ub-PCNA loaded P/T was used, which mimics TLS post-UV stress, neither PDIP38 nor PDIP38^{PM} showed any inhibition of Pol η^{PM} activities (Figure 5C). These results were consistent with GST-fusion protein pull-down assays (Figure 5D). GST-PDIP38 showed direct interaction with Pol η, whereas GST-PDIP38^{PM} showed diminished interaction with Pol η (Figure 5D). Interestingly, the PDIP38-Pol η interaction depended on an intact UBZ domain, as the inclusion of 2 mM EDTA disrupted the binding (Figure 5D).

Inhibition of polymerase activity can arise from two scenarios: direct inhibition of catalysis or exclusion of Pol η from binding to the P/T/PCNA terminus. To distinguish between these possibilities, we determined

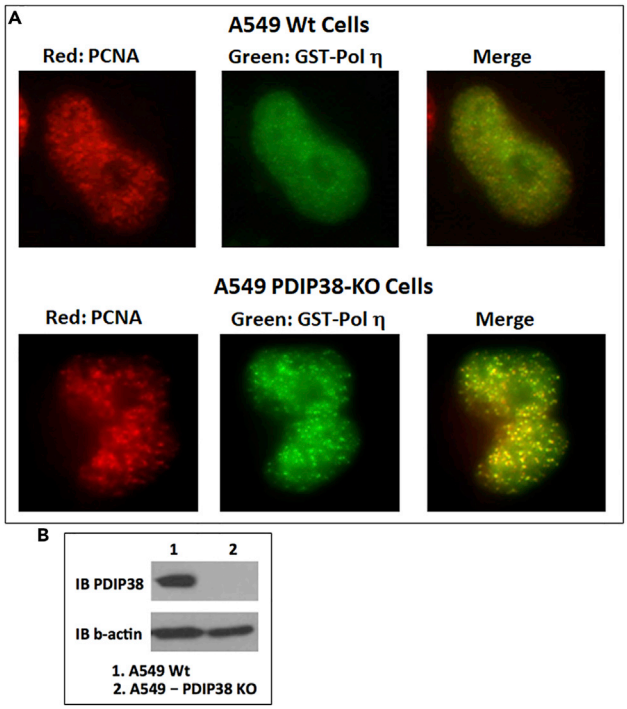

Figure 6. Loss of PDIP38 Leads to Pol η Recruitment to Replication Foci without UV Stress

(A) Parental and PDIP38-null A549 cells were transfected with GFP-Pol η and imaged 36 hr later for localization of Pol η and PCNA. Merge channel shows the superimposition of the GFP (green) and PCNA (red) fluorescence signals.

(B) CRISPR knockout of PDIP38 in A549 cells. β-Actin as loading control is shown.

the impact of increasing concentrations of PDIP38 on Pol η binding to P/T/PCNA terminus (Figure 5E). Synthetic chromatin (P/T/PCNA) was incubated with constant concentrations of Pol η and increasing concentrations of PDIP38 (50–500 nM). The amount of Pol η bound to chromatin was analyzed by western blot analysis (Figures 5E and 5F). Under these conditions, PDIP38 inhibited Pol η binding to the P/T/PCNA terminus in a concentration-dependent manner. By contrast, $PDIP38^{PM}$ had no impact on $Pol\ \eta^{PM}$ binding to P/T/Ub-PCNA terminus (Figures 5G and 5H).

At the cellular level, the hypothesis predicts that, upon loss of sequestration by PDIP38, some Pol η will be recruited to the replication fork and form foci even in the absence of UV irradiation. To test this, we generated PDIP38-null A549 cells by CRISPR methods (Figure 6B). Parental and PDIP38-null cells were then transfected with GFP-Pol η for ectopic expression and visualization. PDIP38-null cells showed significantly more Pol η foci co-localized with PCNA, whereas the parental cells display more diffused green fluorescence, typical of Pol η distribution in non-stressed cells (Göhler et al., 2011; Kannouche et al., 2001, 2004) (Figure 6A).

Collectively these studies show that PDIP38 interaction with Pol η prevents its participation in DNA replication process in the absence of DNA damage. Upon UV irradiation, both PDIP38 and Pol η are phosphorylated by ATR and the phosphorylated forms lose the ability to interact with each other.

DISCUSSION

Mechanism for the Recruitment of Pol η to a Stalled Replication Fork

Our present studies permit a reappraisal of the mechanisms involved in the recruitment of Pol η to stalled replication forks. This is illustrated in Figure 7. In unstressed cells (Figure 7, I), DNA replication fidelity is the sole priority. Consequently, low-fidelity Pol η is sequestered by PDIP38 to prevent its participation in DNA replication. Post-UV exposure, phosphorylation of Pol η by ATR and PKC is necessary and sufficient for its recruitment to the lesion site with monoubiquitinated PCNA regardless of whether the terminus is released from Pol δ (Figure 7, II). The high affinity of phosphorylated Pol η for Ub-PCNA can overcome the binding of

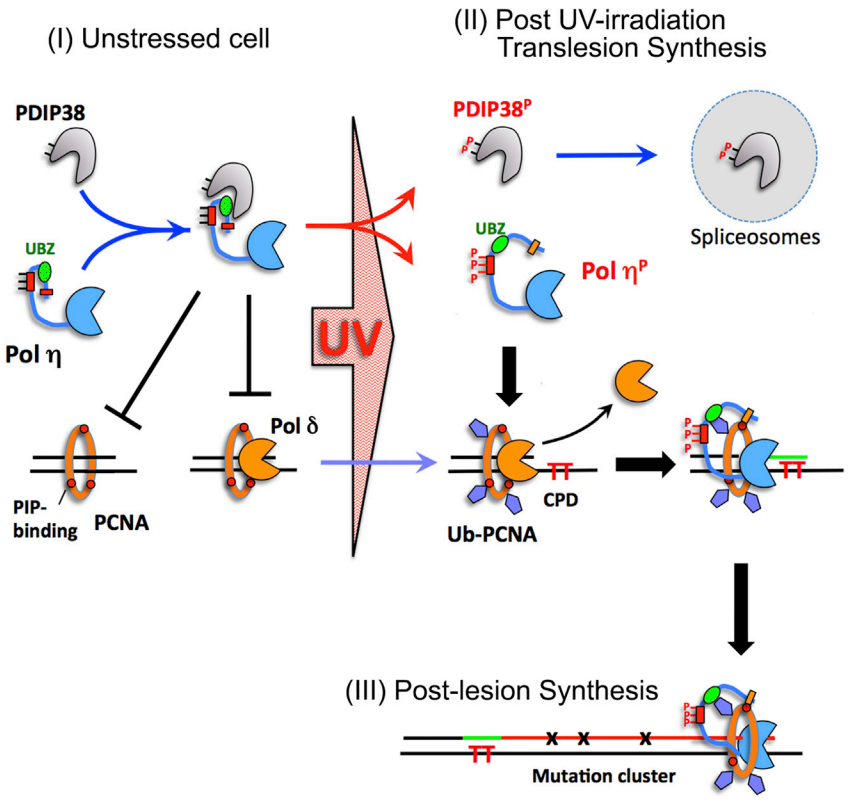

Figure 7. Proposed Model of Pol η Regulation by Phosphorylation and Sequestration

(I) Before DNA damage stress, Pol η is sequestered by PDIP38 away from the replication fork to ensure chromosome duplication is conducted by high-fidelity polymerases. (II) Upon UV irradiation, phosphorylation by ATR and PKC endows Pol η with overpowering affinity toward P/T/Ub-PCNA terminus so that it has sole access to conduct TLS and to maximize cell survival. PDIP38 is shuttled to spliceosomes for alternative splicing. (III) The high affinity between phosphorylated Pol η and Ub-PCNA protects the P/T terminus post-UV stress at the price of mutation clusters.

other molecules that occupy the terminus through the PCNA-PIP interactions. The prompt recruitment of Pol η relieves replication fork stalling and promotes cell survival.

There are multiple potential PIP motifs and Rev1-interacting motif in addition to UBZ domain at the C-terminus of Pol η (Haracska et al., 2001; Pozhidaeva et al., 2012). The PIP motif is required for its translesion function and is most likely the initial anchor for its recruitment to PCNA or Ub-PCNA (Goodman and Woodgate, 2013). Our study suggests that the C-terminal non-catalytic domain of Pol η could adopt different conformations upon phosphorylation. How the PIP motif, Rev1-interacting region, and the UBZ domain interact with each other should be explored further, although caution should be exercised while interpreting the experimental results. Alterations in one of the motifs could very likely alter the conformations of the other motifs.

Exclusion of Pol η from Routine DNA Replication Is as Vital to Cell Fate as Timely Recruitment upon Lesion Encounter

Research on translesion polymerases has focused on the mechanisms that recruit them to the lesion sites and provide subsequent efficacy and specificity in TLS. There is scant information on the exclusion mechanisms that prevent TLS polymerases from unregulated participation in routine DNA replication process, which could result in far direr organismal or cellular fates due to their low fidelity and processivity in replication.

Our studies reveal two avenues that lead to the restriction of Pol η from unwanted participation in routine DNA replication. The first comes from differential affinities of Pol η and its UV-activated form. Pol η has low

activities in terms of being recruited to P/T/PCNA terminus until being phosphorylated by ATR and PKC under the regulation of the DNA damage tolerance pathway (Figure 7, II). It seems likely that activation mutations of Pol η, or deregulation of the control of its phosphorylation, could have significant impact on cell fate. Our studies revealed that ectopic expression of activation mutant of Pol η (Pol η^{PM}) leads to cell death.

The other safeguard involves sequestration by an interacting protein, PDIP38 (Figure 7, I). Our results indicate that a single mechanism regulates both safeguard pathways: ATR phosphorylation induced by UV irradiation (Figure 7). Upon UV irradiation, PDIP38 is phosphorylated by ATR and loses its affinity toward Pol η and hence the ability to sequester. On the other hand, ATR and PKC phosphorylation of Pol η increases its affinity toward Ub-PCNA to facilitate TLS (Figure 7, II). The sequestration mechanism demands that there should be adequate quantity of PDIP38 under cellular conditions to bind Pol η, although it is impossible to assess all cells. In U2OS cells, it is estimated that there are about 70,000 molecules of PDIP38 and less than 500 molecules of Pol η (Beck et al., 2011). However, caution should be taken as most of PDIP38 molecules are localized in the cytosol and mitochondria, although PDIP38 can be shuttled between the nucleus and cytosol (Hernandes et al., 2017).

Our proposed model suggests that loss of either safeguard could lead to a dire consequence: unregulated participation of low-fidelity Pol η in routine DNA replication processes. Indeed, ectopic expression of the phosphomimetic mutant, Pol η^{PM}, leads to cell death. In some respects, Pol η^{PM}-expressing cells have a similar phenotype as primary PDIP38-null fibroblasts in that they can only replicate a few generations before dying (Brown et al., 2014). The lethal phenotype of PDIP38-null mice could originate from multiple functions endowed by PDIP38. It is tempting to suggest that the phenotype of PDIP38-null mice results from Pol η participation in routine DNA replication process. Our study shows that PDIP38 knockout leads to Pol η loading to PCNA foci in the absence of UV irradiation. Consistent with our studies, Tissier et al. demonstrated that PDIP38 knockdown by small interfering RNA also results in increased Pol η foci formation (Tissier et al., 2010) in the absence of UV damage.

The proposed model suggests that overexpression of Pol η^{PM} or suppression of PDIP38 may lead to a mutator phenotype, although these studies are challenging due to the fragile status of the resulting cell lines. The availability of $PCNA^{K164R}$ cell lines (Arakawa et al., 2006; Hendel et al., 2011) used in antibody diversification studies might provide a means for additional investigation. The inability to form Ub-PCNA in these cells might provide resistance to the formation of stable complexes of Pol η or Pol η^{PM} at the replication form and increase the chances of survival.

Implications in Cancer Etiology

The stability of the complex formed between Ub-PCNA and phosphorylated Pol η at the lesion site has important implications in determining which enzyme finishes the post-translesion DNA synthesis on the lagging strand. It raises questions of when or whether the second switch, i.e., Pol δ displacing Pol η post-lesion bypass in the classical TLS model, really occurs. Pol η^{PM} in combination with Ub-PCNA can processively replicate a fragment the size of Okazaki fragment within minutes, as our results showed. Post-UV irradiation, phosphorylated Pol η resides at the foci for a significant duration and is resistant to triton extraction (~10 min) before fixation, in our study and has also been previoulsy reported (Kannouche et al., 2001). That is more than enough time for phosphorylated Pol η to complete the replication the Okazaki fragment. It is interesting to note that in yeast, lack of TLS in S-phase results in DNA gaps in G2 and these are no larger than Okazaki fragments under low to moderate UV exposure (Daigaku et al., 2010). In addition, post-UV stress, both phosphorylated Pol η (Chen et al., 2008; Göhler et al., 2011) and mono-ubiquitinated PCNA exist for significant duration, with Ub-PCNA levels detectible up to 72 hr in MRC5 cells (Niimi et al., 2008). When and how, or if the TLS signals are terminated in S-phase is still to be determined. The fact that post-replication repair can be separated from S-phase (Daigaku et al., 2010) may suggest a more globally activated termination signal in late-S or G2. The high affinity between phosphorylated Pol η and Ub-PCNA can exert a protective role for each individual terminus until all TLS operations are near completion for a more synchronized termination. Our data suggest that phosphorylated Pol η can and likely does replicate rest of the Okazaki fragment post-lesion bypass and introduces mutation clusters in that fragment (Figure 7, III).

Pol η is evolved to counter the effect of the most ancient DNA damaging agent and carcinogen: sunlight. This enzyme is ubiquitously expressed and involved in resolving many other bulky lesions. In fact, it can be

argued that any DNA damage or replication stress that activates the ATR pathway could lead to Pol η participation in gap filling, as ATR activation causes the phosphorylation of Pol η and monoubiquitination of PCNA. The low fidelity of Pol η, estimated at about 1/100 (Chen and Sugiyama, 2017; Johnson et al., 2000), can lead to clusters of mutations. Statistically, if Pol η fills a gap of 100 bases, there is a probability of more than 25% of two or more mutations within the hundred bases following probability mass function of binomial distribution.

$$\text{Probability} = \binom{n}{k} p^k (1-p)^{n-k}$$

where n is the gap size, k is the number of mutations within n, and p is the fidelity of polymerase.

The odds of clustered mutations increase with gap size. In a gap of 150 bases, typical of an Okazaki fragment, the odds increase to about 45% of two or more mutations. Compromises in mismatch repair system could further exacerbate Pol η-induced mutation clusters. Thus, our data suggest a mechanism that could explain the prevalence of Pol η signatures in cancer mutations (Nik-Zainal et al., 2012; Supek and Lehner, 2017).

METHODS

All methods can be found in the accompanying Transparent Methods supplemental file.

SUPPLEMENTAL INFORMATION

Supplemental Information includes Transparent Methods and six figures and can be found with this article online at https://doi.org/10.1016/j.isci.2018.07.009.

ACKNOWLEDGMENTS

This work is supported by NIEHS grant ES014737. Thanks to Thomas Jeitner for proofreading the manuscript. GM02359-hTERT cells are generously provided by Dr. Cordeiro-Stone, University of North Carolina; XP30RO cells are generously provided by Dr. Lehmann, University of Sussex.

AUTHOR CONTRIBUTIONS

Z.Z., C.P., E.Y.C.L., and M.Y.W.T.L. designed the study and analyzed all the data. C.P. performed most of the experiments with assistance from S.Z. and H.Z. A.W. initially identified the PDIP38 phosphorylation by ATR. Z.Z., E.Y.C.L., and M.Y.W.T.L. wrote the manuscript.

DECLARATION OF INTERESTS

The authors declare no conflict of interests.

Received: April 19, 2018
Revised: June 26, 2018
Accepted: July 13, 2018
Published: August 31, 2018

REFERENCES

Acharya, N., Brahma, A., Haracska, L., Prakash, L., and Prakash, S. (2007). Mutations in the ubiquitin binding UBZ motif of DNA polymerase eta do not impair its function in translesion synthesis during replication. Mol. Cell. Biol. *27*, 7266–7272.

Acharya, N., Yoon, J.H., Gali, H., Unk, I., Haracska, L., Johnson, R.E., Hurwitz, J., Prakash, L., and Prakash, S. (2008). Roles of PCNA-binding and ubiquitin-binding domains in human DNA polymerase eta in translesion DNA synthesis. Proc. Natl. Acad. Sci. USA *105*, 17724–17729.

Acharya, N., Yoon, J.H., Hurwitz, J., Prakash, L., and Prakash, S. (2010). DNA polymerase eta lacking the ubiquitin-binding domain promotes replicative lesion bypass in humans cells. Proc. Natl. Acad. Sci. USA *107*, 10401–10405.

Arakawa, H., Moldovan, G.L., Saribasak, H., Saribasak, N.N., Jentsch, S., and Buerstedde, J.M. (2006). A role for PCNA ubiquitination in immunoglobulin hypermutation. PLoS Biol. *4*, e366.

Bai, Y. (2015). Detecting protein-protein interactions by gel filtration chromatography. Methods Mol. Biol. *1278*, 223–232.

Beck, M., Schmidt, A., Malmstroem, J., Claassen, M., Ori, A., Szymborska, A., Herzog, F., Rinner, O., Ellenberg, J., and Aebersold, R. (2011). The quantitative proteome of a human cell line. Mol. Syst. Biol. *7*, 549.

Beeckmans, S. (1999). Chromatographic methods to study protein-protein interactions. Methods *19*, 278–305.

Bertoletti, F., Cea, V., Liang, C.C., Lanati, T., Maffia, A., Avarello, M.D.M., Cipolla, L., Lehmann, A.R., Cohn, M.A., and Sabbioneda, S. (2017). Phosphorylation regulates human pol η stability and damage bypass throughout the cell cycle. Nucleic Acids Res. *45*, 9441–9454.

Bienko, M., Green, C.M., Sabbioneda, S., Crosetto, N., Matic, I., Hibbert, R.G., Begovic, T.,

Niimi, A., Mann, M., Lehmann, A.R., et al. (2010). Regulation of translesion synthesis DNA polymerase eta by monoubiquitination. Mol. Cell *37*, 396–407.

Brown, D.I., Lassegue, B., Lee, M., Zafari, R., Long, J.S., Saavedra, H.I., and Griendling, K.K. (2014). Poldip2 knockout results in perinatal lethality, reduced cellular growth and increased autophagy of mouse embryonic fibroblasts. PLoS One *9*, e96657.

Bruning, J.B., and Shamoo, Y. (2004). Structural and thermodynamic analysis of human PCNA with peptides derived from DNA polymerase-delta p66 subunit and flap endonuclease-1. Structure *12*, 2209–2219.

Chen, Y., and Sugiyama, T. (2017). NGS-based analysis of base-substitution signatures created by yeast DNA polymerase eta and zeta on undamaged and abasic DNA templates in vitro. DNA Repair (Amst) *59*, 34–43.

Chen, Y.W., Cleaver, J.E., Hatahet, Z., Honkanen, R.E., Chang, J.Y., Yen, Y., and Chou, K.M. (2008). Human DNA polymerase eta activity and translocation is regulated by phosphorylation. Proc. Natl. Acad. Sci. USA *105*, 16578–16583.

Choe, K.N., and Moldovan, G.L. (2017). Forging ahead through darkness: PCNA, still the principal conductor at the replication fork. Mol. Cell *65*, 380–392.

Cordonnier, A.M., and Fuchs, R.P. (1999). Replication of damaged DNA: molecular defect in xeroderma pigmentosum variant cells. Mutat. Res. *435*, 111–119.

Cortez, D. (2015). Preventing replication fork collapse to maintain genome integrity. DNA Repair (Amst) *32*, 149–157.

Dai, X., You, C., and Wang, Y. (2016). The functions of serine 687 phosphorylation of human DNA polymerase eta in UV damage tolerance. Mol. Cell. Proteomics *15*, 1913–1920.

Daigaku, Y., Davies, A.A., and Ulrich, H.D. (2010). Ubiquitin-dependent DNA damage bypass is separable from genome replication. Nature *465*, 951–955.

Dick, D.A. (1978). The distribution of sodium, potassium and chloride in the nucleus and cytoplasm of *Bufo bufo* oocytes measured by electron microprobe analysis. J. Physiol. *284*, 37–53.

Garg, P., and Burgers, P.M. (2005). Ubiquitinated proliferating cell nuclear antigen activates translesion DNA polymerases eta and REV1. Proc. Natl. Acad. Sci. USA *102*, 18361–18366.

Göhler, T., Sabbioneda, S., Green, C.M., and Lehmann, A.R. (2011). ATR-mediated phosphorylation of DNA polymerase eta is needed for efficient recovery from UV damage. J. Cell Biol. *192*, 219–227.

Goodman, M.F., and Woodgate, R. (2013). Translesion DNA polymerases. Cold Spring Harb. Perspect. Biol. *5*, a010363.

Guilliam, T.A., Bailey, L.J., Brissett, N.C., and Doherty, A.J. (2016). PolDIP2 interacts with human PrimPol and enhances its DNA polymerase activities. Nucleic Acids Res. *44*, 3317–3329.

Haracska, L., Johnson, R.E., Unk, I., Phillips, B., Hurwitz, J., Prakash, L., and Prakash, S. (2001). Physical and functional interactions of human DNA polymerase eta with PCNA. Mol. Cell. Biol. *21*, 7199–7206.

Hedglin, M., Pandey, B., and Benkovic, S.J. (2016). Characterization of human translesion DNA synthesis across a UV-induced DNA lesion. Elife *5*, https://doi.org/10.7554/eLife.19788.

Hendel, A., Krijger, P.H., Diamant, N., Goren, Z., Langerak, P., Kim, J., Reissner, T., Lee, K.Y., Geacintov, N.E., Carell, T., et al. (2011). PCNA ubiquitination is important, but not essential for translesion DNA synthesis in mammalian cells. PLoS Genet. *7*, e1002262.

Hernandes, M.S., Lassegue, B., and Griendling, K.K. (2017). Polymerase delta-interacting protein 2: a multifunctional protein. J. Cardiovasc. Pharmacol. *69*, 335–342.

Hoege, C., Pfander, B., Moldovan, G.L., Pyrowolakis, G., and Jentsch, S. (2002). RAD6-dependent DNA repair is linked to modification of PCNA by ubiquitin and SUMO. Nature *419*, 135–141.

Johnson, R.E., Prakash, L., and Prakash, S. (2005). Distinct mechanisms of cis-syn thymine dimer bypass by Dpo4 and DNA polymerase eta. Proc. Natl. Acad. Sci. USA *102*, 12359–12364.

Johnson, R.E., Prakash, S., and Prakash, L. (1999). Efficient bypass of a thymine-thymine dimer by yeast DNA polymerase, Poleta. Science *283*, 1001–1004.

Johnson, R.E., Washington, M.T., Prakash, S., and Prakash, L. (2000). Fidelity of human DNA polymerase eta. J. Biol. Chem. *275*, 7447–7450.

Jung, Y.S., Hakem, A., Hakem, R., and Chen, X. (2011). Pirh2 E3 ubiquitin ligase monoubiquitinates DNA polymerase eta to suppress translesion DNA synthesis. Mol. Cell. Biol. *31*, 3997–4006.

Kannouche, P., Broughton, B.C., Volker, M., Hanaoka, F., Mullenders, L.H., and Lehmann, A.R. (2001). Domain structure, localization, and function of DNA polymerase eta, defective in xeroderma pigmentosum variant cells. Genes Dev. *15*, 158–172.

Kannouche, P.L., Wing, J., and Lehmann, A.R. (2004). Interaction of human DNA polymerase eta with monoubiquitinated PCNA: a possible mechanism for the polymerase switch in response to DNA damage. Mol. Cell *14*, 491–500.

Kim, S.T., Lim, D.S., Canman, C.E., and Kastan, M.B. (1999). Substrate specificities and identification of putative substrates of ATM kinase family members. J. Biol. Chem. *274*, 37538–37543.

Krezel, A., and Maret, W. (2006). Zinc-buffering capacity of a eukaryotic cell at physiological pZn. J. Biol. Inorg. Chem. *11*, 1049–1062.

Krezel, A., and Maret, W. (2016). The biological inorganic chemistry of zinc ions. Arch. Biochem. Biophys. *611*, 3–19.

Kunkel, T.A. (2003). Considering the cancer consequences of altered DNA polymerase function. Cancer Cell *3*, 105–110.

Lin, Q., Clark, A.B., McCulloch, S.D., Yuan, T., Bronson, R.T., Kunkel, T.A., and Kucherlapati, R. (2006). Increased susceptibility to UV-induced skin carcinogenesis in polymerase eta-deficient mice. Cancer Res. *66*, 87–94.

Lin, S.H., Wang, X., Zhang, S., Zhang, Z., Lee, E.Y., and Lee, M.Y. (2013). Dynamics of enzymatic interactions during short flap human Okazaki fragment processing by two forms of human DNA polymerase delta. DNA Repair (Amst) *12*, 922–935.

Ma, X., Liu, H., Li, J., Wang, Y., Ding, Y.H., Shen, H., Yang, Y., Sun, C., Huang, M., Tu, Y., et al. (2017). Poleta O-GlcNAcylation governs genome integrity during translesion DNA synthesis. Nat. Commun. *8*, 1941.

Maga, G., Crespan, E., Markkanen, E., Imhof, R., Furrer, A., Villani, G., Hubscher, U., and van Loon, B. (2013). DNA polymerase delta-interacting protein 2 is a processivity factor for DNA polymerase lambda during 8-oxo-7,8-dihydroguanine bypass. Proc. Natl. Acad. Sci. USA *110*, 18850–18855.

Masutani, C., Kusumoto, R., Iwai, S., and Hanaoka, F. (2000). Mechanisms of accurate translesion synthesis by human DNA polymerase eta. EMBO J. *19*, 3100–3109.

Matsuda, T., Bebenek, K., Masutani, C., Rogozin, I.B., Hanaoka, F., and Kunkel, T.A. (2001). Error rate and specificity of human and murine DNA polymerase eta. J. Mol. Biol. *312*, 335–346.

Niimi, A., Brown, S., Sabbioneda, S., Kannouche, P.L., Scott, A., Yasui, A., Green, C.M., and Lehmann, A.R. (2008). Regulation of proliferating cell nuclear antigen ubiquitination in mammalian cells. Proc. Natl. Acad. Sci. USA *105*, 16125–16130.

Nik-Zainal, S., Alexandrov, L.B., Wedge, D.C., Van Loo, P., Greenman, C.D., Raine, K., Jones, D., Hinton, J., Marshall, J., Stebbings, L.A., et al. (2012). Mutational processes molding the genomes of 21 breast cancers. Cell *149*, 979–993.

Oganesyan, N., Ankoudinova, I., Kim, S.H., and Kim, R. (2007). Effect of osmotic stress and heat shock in recombinant protein overexpression and crystallization. Protein Expr. Purif. *52*, 280–285.

Paine, P.L., Pearson, T.W., Tluczek, L.J., and Horowitz, S.B. (1981). Nuclear sodium and potassium. Nature *291*, 258–259.

Pedley, A.M., Lill, M.A., and Davisson, V.J. (2014). Flexibility of PCNA-protein interface accommodates differential binding partners. PLoS One *9*, e102481.

Pozhidaeva, A., Pustovalova, Y., D'Souza, S., Bezsonova, I., Walker, G.C., and Korzhnev, D.M. (2012). NMR structure and dynamics of the C-terminal domain from human Rev1 and its complex with Rev1 interacting region of DNA polymerase eta. Biochemistry *51*, 5506–5520.

Rogozin, I.B., Goncearenco, A., Lada, A.G., De, S., Yurchenko, V., Nudelman, G., Panchenko, A.R., Cooper, D.N., and Pavlov, Y.I. (2018). DNA polymerase eta mutational signatures are found

in a variety of different types of cancer. Cell Cycle *17*, 1–8.

Roos, W.P., and Kaina, B. (2006). DNA damage-induced cell death by apoptosis. Trends Mol. Med. *12*, 440–450.

Rubin, A.F., and Green, P. (2009). Mutation patterns in cancer genomes. Proc. Natl. Acad. Sci. USA *106*, 21766–21770.

Sabbioneda, S., Gourdin, A.M., Green, C.M., Zotter, A., Giglia-Mari, G., Houtsmuller, A., Vermeulen, W., and Lehmann, A.R. (2008). Effect of proliferating cell nuclear antigen ubiquitination and chromatin structure on the dynamic properties of the Y-family DNA polymerases. Mol. Biol. Cell *19*, 5193–5202.

Sabbioneda, S., Green, C.M., Bienko, M., Kannouche, P., Dikic, I., and Lehmann, A.R. (2009). Ubiquitin-binding motif of human DNA polymerase eta is required for correct localization. Proc. Natl. Acad. Sci. USA *106*, E20, author reply E21.

Segurado, M., and Tercero, J.A. (2009). The S-phase checkpoint: targeting the replication fork. Biol. Cell *101*, 617–627.

Silverstein, T.D., Johnson, R.E., Jain, R., Prakash, L., Prakash, S., and Aggarwal, A.K. (2010). Structural basis for the suppression of skin cancers by DNA polymerase eta. Nature *465*, 1039–1043.

Supek, F., and Lehner, B. (2017). Clustered mutation signatures reveal that error-prone DNA repair targets mutations to active genes. Cell *170*, 534–547 e523.

Tissier, A., Janel-Bintz, R., Coulon, S., Klaile, E., Kannouche, P., Fuchs, R.P., and Cordonnier, A.M. (2010). Crosstalk between replicative and translesional DNA polymerases: PDIP38 interacts directly with Poleta. DNA Repair (Amst) *9*, 922–928.

Washington, M.T., Johnson, R.E., Prakash, L., and Prakash, S. (2003). The mechanism of nucleotide incorporation by human DNA polymerase eta differs from that of the yeast enzyme. Mol. Cell. Biol. *23*, 8316–8322.

Watanabe, K., Tateishi, S., Kawasuji, M., Tsurimoto, T., Inoue, H., and Yamaizumi, M. (2004). Rad18 guides poleta to replication stalling sites through physical interaction and PCNA monoubiquitination. EMBO J. *23*, 3886–3896.

Waters, L.S., Minesinger, B.K., Wiltrout, M.E., D'Souza, S., Woodruff, R.V., and Walker, G.C. (2009). Eukaryotic translesion polymerases and their roles and regulation in DNA damage tolerance. Microbiol. Mol. Biol. Rev. *73*, 134–154.

Wong, A., Zhang, S., Mordue, D., Wu, J.M., Zhang, Z., Darzynkiewicz, Z., Lee, E.Y., and Lee, M.Y. (2013). PDIP38 is translocated to the spliceosomes/nuclear speckles in response to UV-induced DNA damage and is required for UV-induced alternative splicing of MDM2. Cell Cycle *12*, 3184–3193.

Woodruff, R.V., Bomar, M.G., D'Souza, S., Zhou, P., and Walker, G.C. (2010). The unusual UBZ domain of Saccharomyces cerevisiae polymerase eta. DNA Repair (Amst) *9*, 1130–1141.

Yagi, Y., Ogawara, D., Iwai, S., Hanaoka, F., Akiyama, M., and Maki, H. (2005). DNA polymerases eta and kappa are responsible for error-free translesion DNA synthesis activity over a cis-syn thymine dimer in *Xenopus laevis* oocyte extracts. DNA repair (Amst) *4*, 1252–1269.

Zhao, Y., Biertumpfel, C., Gregory, M.T., Hua, Y.J., Hanaoka, F., and Yang, W. (2012). Structural basis of human DNA polymerase eta-mediated chemoresistance to cisplatin. Proc. Natl. Acad. Sci. USA *109*, 7269–7274.

ISCI, Volume *6*

Supplemental Information

Phosphorylation Alters the Properties of Pol η: Implications for Translesion Synthesis

Chandana Peddu, Sufang Zhang, Hong Zhao, Agnes Wong, Ernest Y.C. Lee, Marietta Y.W.T. Lee, and Zhongtao Zhang

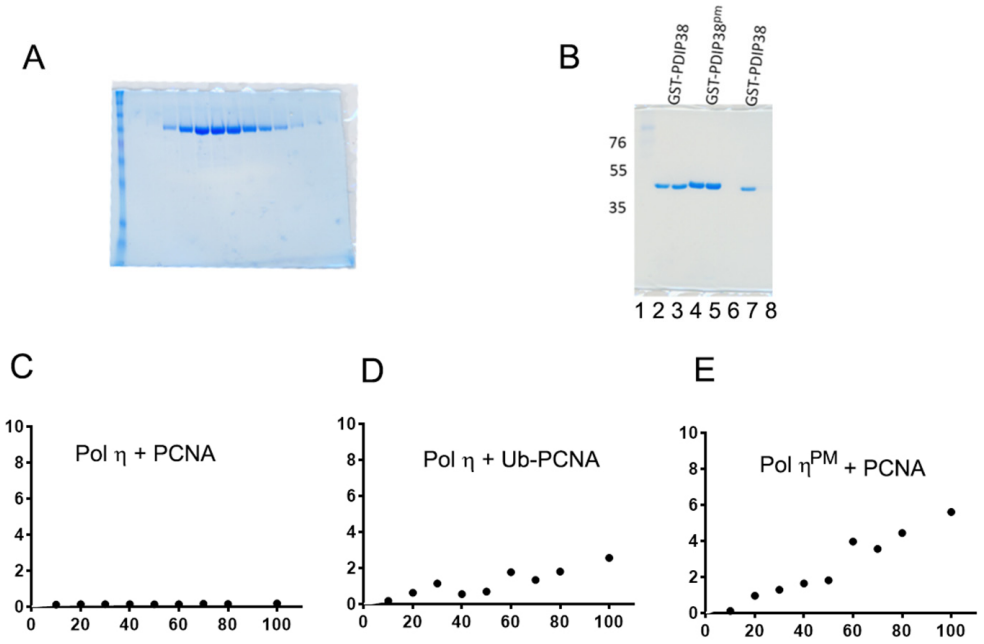

Figure S1, related to Figure 1. Purified recombinant proteins and quantification of titration studies.

(A) SDS-PAGE of purified Pol η post-gel-filtration chromatography on HiLoad 26/600 Superdex 200 pg column (GE Healthcare). (B) SDS-PAGE of purified recombinant GST-tagged PDIP38 and its phosphomimetic mutant, GST-PDIP38^{PM} on beads (lanes 2-5) or eluted fractions (lanes 6-8, collected fractions of glutathione elution). (C-E) Quantification of Figure 1F in same scale as in Figure 1G.

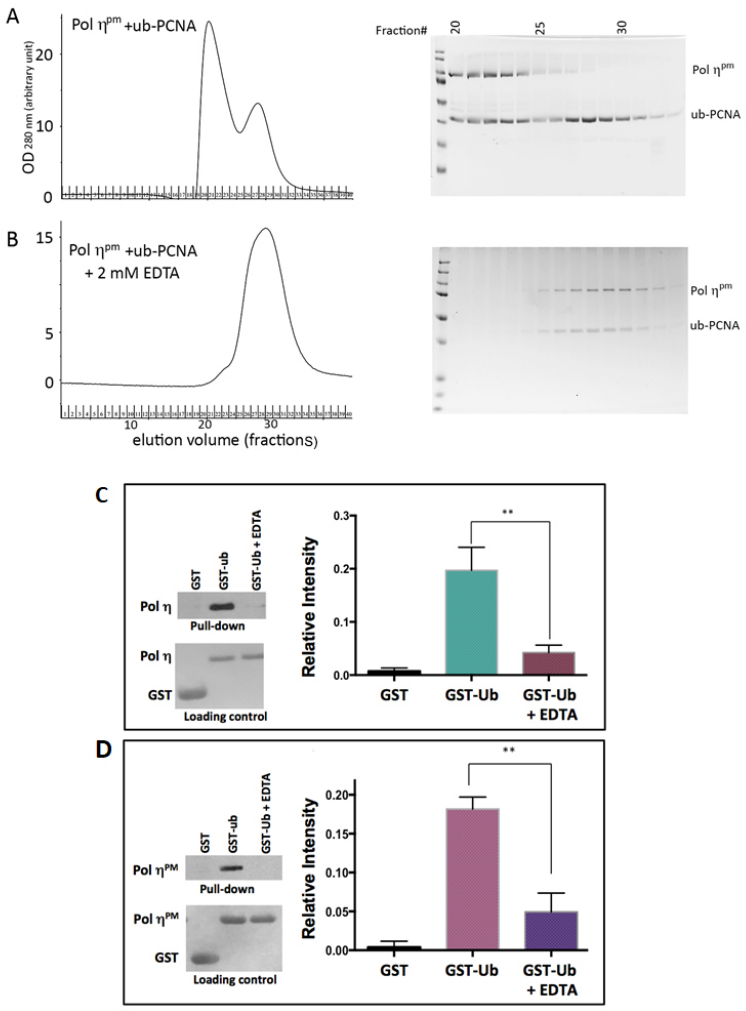

Figure S2, related to Figure 2. Intact UBZ domain is essential for high affinity binding between Pol η^{PM} and Ub-PCNA. This figure is related to Figure 2.
(A) Pol η^{PM} and Ub-PCNA forms a complex that co-eluted on gel-filtration column (Superdex 200 10/300 GL). This is the same figure as figure 2C. (B) Inclusion of 2 mM EDTA disrupts the tight binding of Pol η^{PM} with Ub-PCNA. Protein contents of fractions post gel-filtration were analyzed by SDS-PAGE and visualized by Coomassie staining. (C-D) Western Blot of recombinant Pol η and Pol η^{PM} pulled down by GST-tagged ubiquitin in the absence and presence 2 mM EDTA. GST alone serves as a negative control and Ponceau staining of GST-Ub as a loading control. Relative protein amount was quantified using ImageJ and data shown as mean ± SD of 3 individual experiments and differences between groups analyzed by unpaired t-test. ** indicates $P \leq 0.01$.

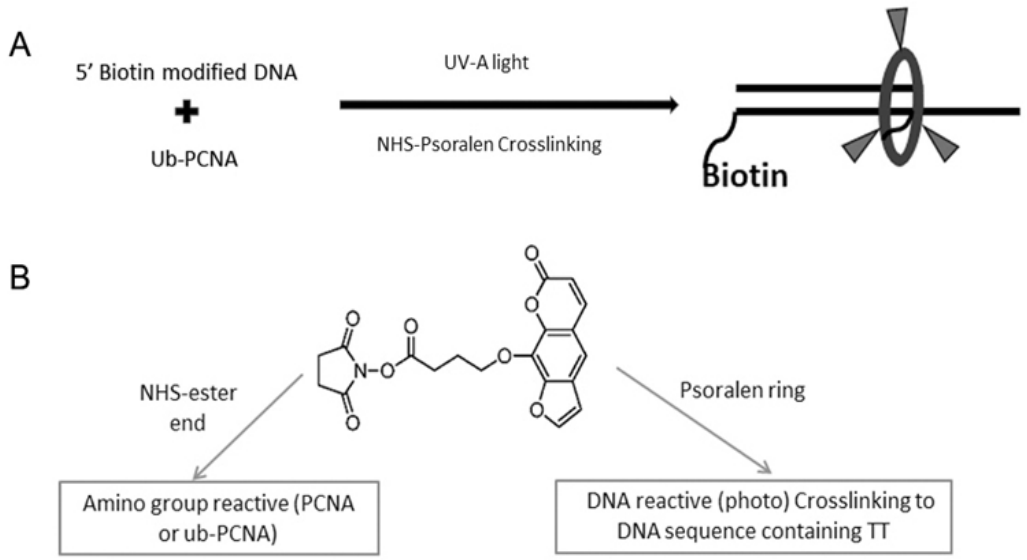

Figure S3, related to Figure 3. Schematic representation for preparation of the synthetic chromatin. This figure is related to Figure 3.

(A-B) Synthetic chromatin with monoubiquitinated-PCNA (Ub-PCNA) loaded at the primer/template (p/t) end. NHS-Psoralen (succinimidyl-[4-(psoralen-8-yloxy)]-butyrate) was used as the crosslinker. NHS-Psoralen can react with amino group (Ub-PCNA) on one end while react with DNA upon UV irradiation (UV-A) on the other.

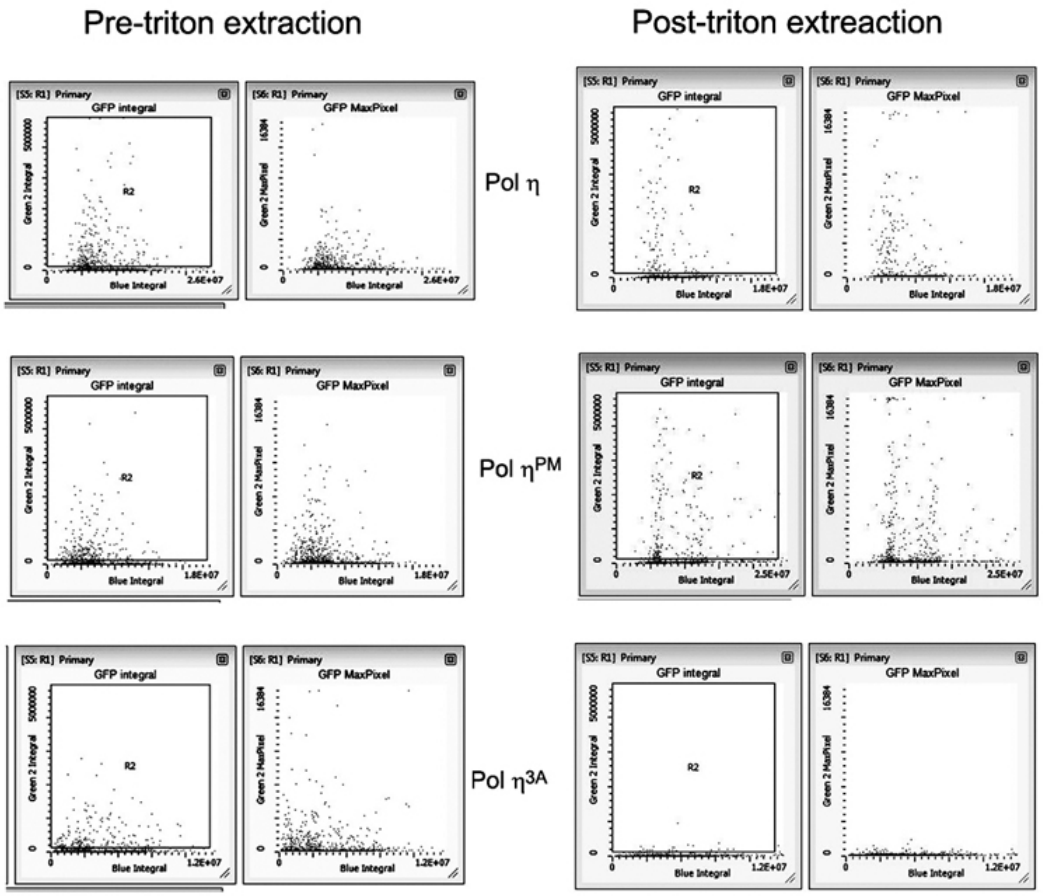

Figure S4, related to Figure 4. Efficient retention of Pol η on UV-induced damage foci requires phosphorylation. This figure is related to Figure 4.

Whole cell population was analyzed for GFP-Pol η signal after UV damage by laser scanning cytometry. MRC5-SV2 cells were transfected with GFP-Pol η, GFP-Pol η^{PM}, or GFP-Pol η^{3A} and irradiated by 30 J/m^2 of UV. After 5 hours, GFP signals were analyzed pre- and post-triton extraction. The GFP signals were read in pixels as integrated per cell basis (GFP integral, signal retained by all foci in a cell), or the highest signal within each cell (MaxPixel, intensity of the strongest foci).

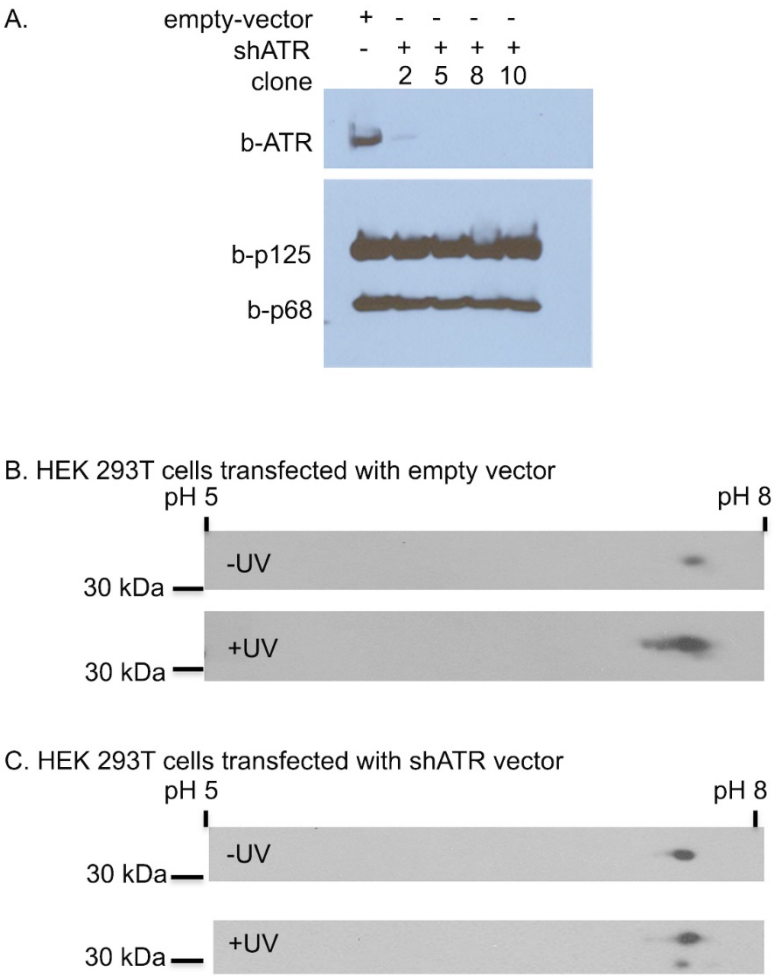

Figure S5, related to Figure 5. PDIP38 is post-translationally modified by the ATR kinase after UVC irradiation. (A) ATR knockdown by shRNA in HEK293T cells. HEK293T cells were transfected either with empty vector or shRNA targeting ATR. Stable clones were selected by antibiotic. ATR suppression was detected by Western blot analysis. Clone 10 is selected for subsequent studies. (B) HEK293T cells were subjected to global UVC irradiation at a dose of 60 J/m^2. The nuclear protein fraction from non-UV-treated cells as well as UV treated cells were isolated and subjected to isoelectric focusing for the first dimension (IPG strips with pH range 5-8) and separated on a 10% SDS-PAGE for the second dimension. Subsequently Western blot analysis using anti-PDIP38 antibody was used to determine modified isoforms of PDIP38. Phosphorylated isoforms of PDIP38 were detected in UV irradiated cells. (C) Phosphorylated isoforms of PDIP38 were not detected in ATR knockdown (shATR) cells after UVC irradiation.

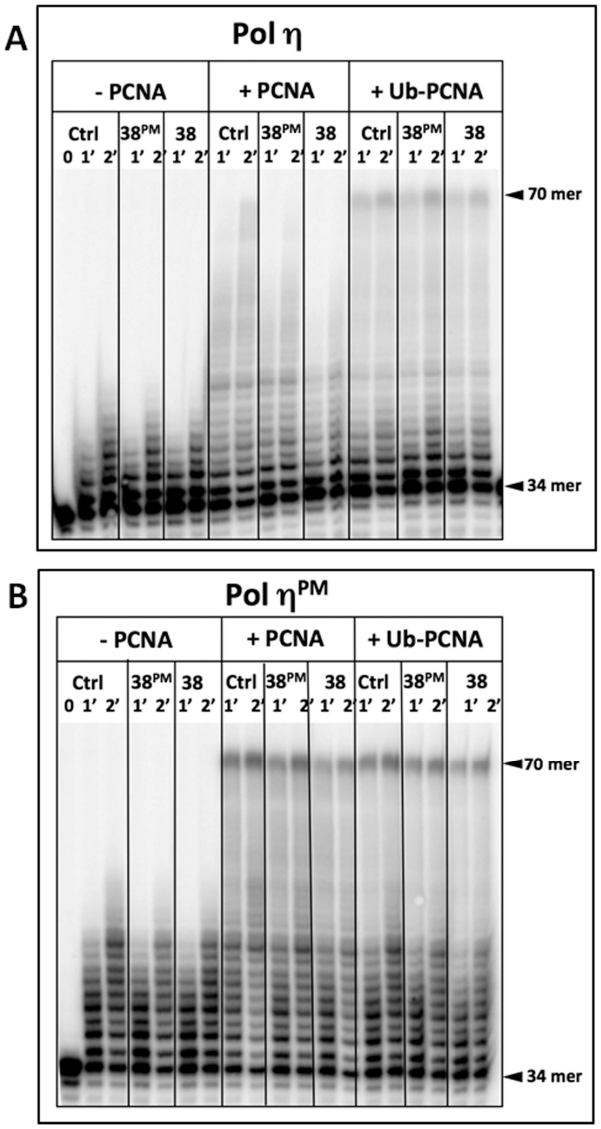

Figure S6, related to Figure 5. PDIP38 inhibits Pol η activity in oligo extension while PDIP38^{PM} shows no effect. This figure is related to Figure 5.

(A) Pol η activity is inhibited in the presence of PDIP38. Representative sequencing gel showing resolved extension products of Pol η on P/T alone (-PCNA), PCNA or Ub-PCNA preloaded P/T (+PCNA) or (+Ub-PCNA) at 1 min and 2 mins. (Ctrl) Indicates control lane; (38) indicates reaction performed in the presence of 200 nM of PDIP38; (38^{PM}) indicates reaction performed in the presence of 200 nM of phosphomimetic mutant of PDIP38. (B) Activity of Pol η^{PM} is not affected by the presence of PDIP38. Representative sequencing gel showing resolved extension products of Pol η^{PM} on PCNA or ub-PCNA-preloaded p/t at 1 min and 2 mins. (Ctrl) Indicates control lane; (38^{PM}) indicates reaction performed in the presence of 200 nM of phosphomimetic mutant of PDIP38; (38) indicates in presence of 200 nM of PDIP38.

Transparent Methods

Constructs for expression and purification of recombinant Pol η

The coding region for full-length Pol η was cloned into pET22b vector between Nde I and Xho I sites with the initiation codons coinciding with Nde I restriction site and the stop-codon eliminated to generate C-terminal 6-Histidine tag from vector. Mutagenesis of three phosphorylation sites was sequentially constructed with QuickChange Site-Directed Mutagenesis Kit (Agilent). All single and combinatorial double mutants were generated and constructs were subsequently sequenced. The resulting construct was transformed into *E coli* (Resetta 2) containing an ubiquitin expressing plasmid (pET28b). *E. Coli* was grown overnight at 37°C in LB media before dilution (1 to 40) into TB with antibiotics (100 μg/ml ampicillin and 50 μg/ml Kanamycin) and grown at 30°C until culture reached an O.D.600 value of 1.0. IPTG was added to 1 mM and the incubation was continued at 22°C overnight before harvesting. Pellet from 1 litre culture (~10 g) was suspended in about 50 ml lysis buffer (50 mM phosphate buffer, pH 7.0, 0.5 M NaCl, 10 mM benzamidine, 0.25% triton X-100, 10 mM mercaptoethanol and 5 mM imidazole) and lysed by sonication (30 s burst at 80% power, 3 to 4 times on ice). Cell lysates were clarified by centrifugation at 21000 rpm for 60 minutes with Beckman 45 T1 Rotor. The supernatant were then loaded onto an 8 ml His-Select (Sigma) column pre-charged with Zn^{2+} at flow rate of 0.5 ml/min. The column was washed with 100 ml lysis buffer (2 ml/min) after loading. Bound protein was eluted in 30 ml by elution buffer (20 mM HEPES, pH 7.5, 250 mM NaCl, 10 mM mercaptoethanol, and 200 mM imidazole). Subsequently, the eluent was applied to a 5-ml Hi-Trap Heparin column (GE Healthcare) pre-equilibrated with buffer A (20 mM HEPES, pH 7.5, 250 mM NaCl, 10% glycerol, 10 mM mercaptoethanol). Pol η was then eluted by a linear gradient of NaCl from 0.25 M to 1 M with FPLC (buffer A to B. Buffer B: 20 mM HEPES, pH 7.5, 1 M NaCl, 10% glycerol, 10 mM mercaptoethanol) in 40 fractions (1ml/min, 1 ml per fraction). Fractions with the highest concentration of Pol η (6-7 fractions, 400 to 550 mM NaCl) were pooled and concentrated to less than 2 ml. The resulting sample was then applied to Gel filtration column (HiLoad Superdex 200 pg, 26/60, GE) equilibrated with buffer C (15 mM citrate, pH 6.5, 0.3 M NaCl, 1 mM DTT, 10% glycerol). Protein was eluted at 0.5 ml/min with 2 ml fraction size. Purified Pol η was aliquoted and flash frozen with liquid nitrogen and stored at -80°C.

Expression and purification of other recombinant proteins

Fragment coding for residue 51 to 368 of PDIP38 was amplified by PCR and inserted into pET-sumo and pGEX-2T vectors for recombinant protein production. Resulting plasmids were transfected into *E coli* (Rosetta, DE3, pLys) with corresponding antibiotic selection. For protein production, cells were grown over night in LB media with 0.5 M NaCl at 37°C. Overnight culture was then diluted 1:50 into fresh LB media with 0.5 M NaCl and 1 mM betaine and grew until the O. D. 600 of 0.6–0.8. IPTG was added to final concentration of 1 mM after cells were cooled to 22°C for overnight induction. Cells were then harvested by centrifugation next morning and stored at -80°C. Pellet from 1liter culture (sumo-PDIP38, ~5 g) was suspended in about 30 ml lysis buffer (50 mM phosphate buffer, pH 7.0, 0.5 M NaCl, 10 mM benzamidine, 0.25% triton X-100, 10 mM mercaptoethanol and 30 mM imidazole) and lysed by sonication (30s burst at 80% power, 3 to 4 times on ice). Cell lysates were clarified by centrifugation at 21000 rpm for 60 minutes with Beckman 45 T1 Rotor. The supernatant was then loaded onto a 5 ml Hi-trap chelating column pre-charged with Ni^{2+} at flow rate of 1 ml/min. The column was washed with 100 ml lysis buffer (2 ml/min) after loading. Bound protein was eluted in 30 ml by elution buffer (20 mM HEPES, pH

7.5, 250 mM NaCl, 10 mM mercaptoethanol, and 200 mM imidazole). The eluted protein was then added 1 mg sumo specific isopeptidase 1 (SENP1) and the resulting mixture was dialyzed against 1-liter buffer (20 mM TRIS, pH 8.0, 200 mM NaCl, and 5 mM mercaptoethanol) overnight. His-tagged sumo was then removed by binding to 2 ml Ni-NTA beads and the supernatant was applied to Mono-Q column. Recombinant PDIP38 was eluted as a single peak at about 200 mM NaCl. For GST-fusion PDIP38 production, the cell pellet (~5g from 1 liter culture) was lysed in lysis buffer (20 mM HEPES, pH 7.5, 200 mM NaCl, 0.5% triton X-100, 1 mM DTT, and 1 mM EDTA). Cleared supernatant post-centrifugation was added to 1 ml glutathione beads (Sigma) and incubated for 2 hours. After wash with lysis buffer, half of the beads was stored and the other half was eluted with 100 mM reduced glutathione. All samples were stored at -80°C.

Preparation of synthetic chromatin mimicking DNA replication and repair termini

Biotinylated template (3'-biotin-TGCAAAATAGGAGGGGATGGAATAAA-5') was annealed to primer (5'-ACGTTTTATCCTCCCCTAC-3') in PBS buffer at 200 μM concentration. Since psoralen preferentially binds to double stranded DNA grooves formed by T/A pairing and reacts with pyrimidine bases, we designed the template/primer pair with a single stretch of T/A bases (TTTT/AAAA) for crosslinking with PCNA or Ub-PCNA. There are 13 base pairs after the modification site to allow polymerase binding as suggested by the crystal structure of Pol δ and Pol η. The annealed oligos were mixed with Ub-PCNA in 2 ml borate buffer (20 mM, pH 8.5) to final concentration of 20 μM (oligo) and 10 μM (Ub-PCNA) in a 6-well plate on ice. Succinimidyl-[4-9psoralen-8-yloxy0]-butyrate (SPB) was added to a final concentration of 0.5 mM from a 100 mM stock in DMSO. The mixture was incubated on ice for 15 min before irradiation by UVA at 365 nm for 10 minutes. The samples were further irradiated twice for 10 minutes with 30 minutes intervals in between. The resulting sample was then applied to SUPERDEX 200 pg (16/60) column equilibrated with PBS buffer. Excess oligo was separated from cross-linked template/primer/Ub-PCNA and unmodified Ub-PCNA due to size differences. Fractions containing a mixture of crosslinked template/primer/Ub-PCNA and unmodified Ub-PCNA were pooled and subsequently separated by immobilized streptavidin beads. The cross-linking of template/primer/PCNA was conducted in identical protocol with increased concentration (20 μM oligo and 40 μM PCNA). The binding capacities of both beads were determined by increasing concentrations of either Pol η or Pol δ4 until saturation as determined by western-blot analysis.

Oligo Extension assay

The standard reaction buffer contained 50 mM Tris-Cl pH 7.5, 5 mM $MgCl_2$, 50 mM NaCl, 150 mM KCl, 2 mM dithiothreitol, 100 μg/mL BSA, 40 μM dNTPs and 0.5 mM ATP. ^{32}P radiolabelled 34 mer annealed to 70 mer was used as a substrate. Annealed biotin end-modified 70 mer/34 mer was incubated with streptavidin (New England Biolabs, MA) in an excess of 1:1.2 at 37°C for an hour before use to block the ends. Enzymes were diluted in a dilution buffer containing 50 mM Tris-Cl pH 7.5, 4 mM dithiothreitol, 200 μg/mL BSA, 30 mM NaCl and 10% glycerol (v/v). DNA was preloaded with PCNA or Ub-PCNA at 37°C for 5 minutes according to the following reaction mix: 10 mM Tris-Cl pH 7.5, 0.2 mM ATP, 2 mM $MgCl_2$, 6 mM NaCl, 50 mM DNA, 60 nM RFC, and 40 nM PCNA or 40 nM Ub-PCNA. Reactions were then incubated on ice for 5 minutes with respective polymerases (Pol η / Pol η^{PM}) before addition of mix containing all four dNTPs (40 μM) and $MgCl_2$ (5 mM) to start the reaction in a final volume of 30 μL. Reactions were performed at 37°C and reaction aliquots (11 μL) terminated at different time points by addition of 7.5 μL of loading/stop buffer (25 mM EDTA in 95% formaldehyde, 0.01% bromophenol blue and 0.01%

xylene cyanol) and heated at 95°C for 5 minutes to denature. Extension products were then resolved by electrophoresis on 18% polyacrylamide (acrylamide/bisacrylamide 19:1) 8 M urea denaturing gel using Sequi-Gen GT Sequencing Cell (Bio-Rad, CA). Resolved products were visualized by Molecular Dynamics Storm Phosphorimaging system (Amersham Biosciences, NJ). Full-length extension products (70 mer) were expressed as a percentage of the substrate available in respective reactions. For titration studies, the substrate concentrations were maintained constant by using biotin-blocked primer/template (50 nM) that were preloaded by PCNA (40 nM) OR Ub-PCNA (40 nM) using RFC (60 nM). Polymerases (Pol η / Pol η^{PM}) were then added against the substrate at varying concentrations from 0 nM to 100 nM and incubated on ice for 5 minutes before starting the reaction at 37°C by addition of mix containing all four dNTPs (40 μM) and $MgCl_2$ (5 mM) to start the reaction in a final volume of 15 μl. Reaction aliquots (11 μl) were then quenched with 7.5 μl of loading/stop buffer (25 mM EDTA in 95% formaldehyde, 0.01% bromophenol blue and 0.01% xylene cyanol). Extension products were denatured at 95°C for 5 minutes to be separated by 18% polyacrylamide (acrylamide/bisacrylamide 19:1) 8M urea denaturing gel. Fraction of the total substrate that was extended to full-length extension products (70 mer) were quantified and fitted to non-linear regression against enzyme concentration by GraphPad Prism 6.0 (La Jolla, CA), using one-site binding kinetics, to determine apparent K_d from the plotted saturation curves. The sequences of the corresponding oligos are as follows: 70mer: 5' -/5Biosg/ CCT ATC TGA GCA CTA TCA TCG GTC GCA TCG TTG GCT GAA ATC GTG CTG TAG TGG CTG AAT CCC AAC CAA C/3Bio/ -3'; 34mer: 5' – GTT GGT TGG GAT TCA GCC ACT ACA GCA CGA TTT C -3'; Biotin-26-Temp: 5' – AAA TAA GGT AGG GGA GGA TAA AAC GT [Biotin-Q] – 3'; Biotin-Primer: 5' – ACG TTT TAT CCT CCC CTA C – 3'.

Binding of polymerase to synthetic chromatin

Streptavidin immobilized primer/template (P/T) that was cross-linked either with PCNA or Ub-PCNA was assayed to bind recombinant Pol δ either in the presence of purified Pol η or Pol η^{PM}. Corresponding control reactions were also set up with individual proteins to estimate binding capacity. Each reaction had 500 ng of individual protein and was incubated with the immobilized P/T at a binding capacity of 200 ng per reaction in a final reaction mix volume of 200 μL. Assay buffer containing 10 mM HEPES pH 7.5, 15 mM citrate, 1 μM $ZnCl_2$, 40mM NaCl, 160 mM KCl, 1mg/mL BSA, 5% glycerol and 1mM dithiothreitol was used. After incubation at 4°C for 2 hours, the immobilized streptavidin beads were spun down and subsequently washed for at least 3 times. For PCNA immobilized P/T, PBS was used for washing, whereas for Ub-PCNA immobilized, subsequent washes were carried out in the 1X assay buffer. Beads were then boiled in 1X SDS dye (50 mM Tris-HCl pH 6.8, 2% SDS, 10% glycerol, 1% β-mercaptoethanol, 12.5 mM EDTA, 0.02 % bromophenol blue) at 95°C for 5 min. Bound proteins were then resolved by SDS-PAGE and western blot. P/T cross-linked with Ub-PCNA was used to set up a titration assay to determine the relative amounts of Pol η^{PM} or Pol δ bound in the assay buffer mentioned above. In each reaction immobilized P/T at a binding capacity of ~100 ng was incubated with 500 ng of Pol $\eta^{\mathbf{PM}}$ and increasing concentration of Pol δ (500 ng, 1 μg, 1.5 μg, 2 μg, 2.5 μg) for 2 hours at 4°C. Control reactions contained ~100 ng immobilized P/T incubated with either Pol $\eta^{\mathbf{PM}}$ (500 ng) or Pol δ (500 ng) individually. Beads were then spun down and subsequently washed in 1X assay buffer 5 times and bound proteins analyzed by SDS-PAGE and western blot as described above. In order to determine the ability of PDIP38 to sequester Pol η, titration study was performed using the immobilized P/T and recombinant purified PDIP38 and its phosphomimetic mutant, $PDIP38^{PM}$ in two distinct reaction conditions. To mimic conditions of DNA replication, immobilized P/T cross-linked with PCNA was incubated with 500ng of Pol η and titrated with increasing concentrations

of PDIP38 (50, 100, 200, 400, 500 nM). To reflect conditions of DNA repair, immobilized P/T cross-linked with Ub-PCNA was incubated with 500 ng of Pol η^{PM} and titrated with increasing concentrations of PDIP38^{PM} (50, 100, 200, 400, 500 nM). The assay buffer composition as well as incubation, washing and subsequent analysis were performed under the same conditions described above.

GST-fusion protein pull-down assays

For pull down assays, the bait was expressed as a GST – tagged protein bound to glutathione-agarose beads and incubated with either purified recombinant protein or nuclear extract to detect interacting partners. A GST negative control experiment was also set up to rule out GST mediated interaction. The standard reaction mix contained 25 mM HEPES pH 7.5, 50mM NaCl, 160 mM KCl, 0.1 mg/mL BSA, 10% glycerol, 0.25% Triton X-100, 10 mM citrate, 5 μM $ZnCl_2$ and 1mM dithiothreitol unless otherwise specified. HEK 293T nuclear proteins were collected as described above in nuclear extraction buffer (15 mM Tris.Cl pH 7.5, 0.4 M NaCl, 10% (w/v) sucrose, 1 mM DTT) and diluted to reduce the salt concentration to 0.2 M NaCl. GSH-agarose beads with bound GST- (bait protein) were pre-equilibrated with pull down buffer before adding 500 ng of purified protein or 300 μg of nuclear extract and incubated on a shaker at 4°C for 2 hours. Beads were then collected by spinning down at a low speed of 4000 rpm for 1 min and consecutively washed three times in PBS. Bound proteins to bait protein were then collected by boiling in 1X SDS loading buffer (0.1% 2-mercaptoethanol, 0.0005% bromophenol blue, 10% Glycerol, 2% SDS, 63 mM Tris-Cl, pH 6.8) and later analyzed by western blot.

Ectopic expression of proteins in mammalian cells

Pol η cloned into pAcGFP-C1 to be expressed as a C-terminal fusion product of GFP was used to transfect HEK 293T by using lipofectamine 3000 (Thermo fisher, NJ). Simultaneously corresponding phosphorylation deficient mutant GFP-Pol η^{3A} and the phosphomimetic mutant GFP-Pol η^{PM} were also transfected to study the impact of phosphorylation on Pol η localization. Poly-L-lysine (Sigma-Aldrich, MO) coated coverslips were used to plate the cells 36 hrs before transfections to achieve 80% confluence. The next day, cells were rinsed once with PBS and replenished with antibiotic-antimycotic free media and transfected with lipofectamine 3000. Optimized conditions were chosen for transfection of HEK-293T for a well in a 6-welled culture dish. After 6 hours, the media containing the transfection complexes was replaced with fresh media and GFP expression confirmed 36 hours later. SV40- transformed MRC-5 lung fetal fibroblasts, MRC-5 SV2 (Sigma-Aldrich, MO), were also used to study localization of GFP-tagged Pol η and its mutants. FuGENE HD (Promega, WI) was used to transfect these fibroblasts according to the manufacturers protocols. The transfection complexes were added to 3 mL of antibiotic-antimycotic free media and GFP expression was confirmed about 48 hours later. Cells were rinsed once in ice-cold PBS on ice before subsequent fixation and imaging. Control A549 and CRISPR/Cas9 PDIP38 KO A549 cells were plated on Poly-L-lysine coated coverslips 24 hours prior to transfection to achieve 80% confluency at the time of transfection. Lipofectamine 2000 (Thermo fisher, NJ) was used to transfect GFP-tagged Pol η according to manufacturer's protocol. Media containing the transfection complexes was replaced 6 hours later and cells were replenished with fresh media. GFP expression was confirmed 36 hours later and cells were subsequently fixed for imaging.

Immunofluorescence assays

HEK 293T and MRC-5 SV2 cells transiently expressing GFP-tagged Pol η and its mutants, GFP-η^{PM} and GFP- η^{3A}, were exposed to UV-C irradiation to study the effect of UV damage on

localization of Pol η. A dose of 30 J/m^2 of UVC (254 nM) was delivered using UVLMS-38EL series 3 UV lamp with a fluence rate of 2 J/m^2/s. On confirming GFP signal under Axiovert 200M fluorescent microscope (Carl Zeiss, DE) cells were washed once with PBS before UV irradiation and then allowed to recover in replenished media for 5 hours. Cells were then rinsed once in ice-cold PBS before subsequent steps. Cells were fixed either in 4% paraformaldehyde at room temperature for 15 minutes or in 100% methanol at -20° C for 20 minutes. Depending on antibody optimized protocols, cells were permeabilized by using either 0.1% Triton X-100 in PBS at room temperature for 15 minutes or 100% acetone at -20°C for 0.5 min. Subsequently cells were blocked in 5% BSA in PBS at room temperature for 1 hour before incubating in primary antibody overnight at 4° C. Cells were washed three times with PBS and then incubated in fluorescent dye conjugated secondary antibody (Life technologies, CA) for 1 hour at 4° C. To study the chromatin bound fraction cells were subjected to pre-extraction in protease/phosphatase inhibitor (HALT 100X protease phosphatase inhibitor cocktail, EDTA free) supplemented 1% Triton X-100 for 8 minutes at room temperature before fixation to get rid of soluble protein fraction. Protocol was adapted from Kannouche *et al.* (Kannouche et al., 2001). Supernatant containing the extracted protein fraction is removed and rinsed once with PBS before fixation as described above. Cells were then washed with PBS for 3 times before staining with DAPI (Life technologies, CA) at 1 μg/ μL for 15 minutes at room temperature before a final wash and mounting using Prolong Diamond Antifade (Thermo fisher, NJ) onto slides. Slides were imaged using Nikon Eclipse Ti and images captured using NIS Elements Imaging Software, version 4.60.

Cell analysis by Laser Scanning Cytometry

Cells were maintained on coverslips and mounted onto slides using Prolong Diamond Antifade, similar to the protocols followed for imaging of immunofluorescence. After transfection and confirming the GFP signal 36 hours later, one set of cells were fixed with 4% paraformaldehyde while another set was subjected to pre-extraction in 1%Triton X-100 before subsequent fixation. Cellular DNA was counterstained with DAPI. Green fluorescence (GFP) representing GFP-tagged Pol η and its mutants as well as the blue emission of the DAPI-stained DNA were quantified using LSC (iCys; CompuCyte, Westwood, MA) with standard filter settings. Fluorescence was excited using helium-neon (633 nm), argon (488 nm) and violet (405 nm). DAPI staining was used to define the nucleus and set the primary contour for all experiments. At least 3000 cells were counted for each condition; the intensities of GFP max pixel and integrated GFP fluorescence were measured and recorded for each cell. No electronic compensation for possible spectral overlap was applied. For further details of the cell analysis refer to Zhao *et al.* (Zhao, Rybak, Dobrucki, Traganos, & Darzynkiewicz, 2012)

Quantification and Statistical Analysis

Western Blots and Sequencing gels were quantified using ImageJ. All datasets were performed with a $n \geq 3$ and are presented as mean ± the standard error of the mean (SEM). Differences between groups were analysed using unpaired t-test and respective p values were calculated. Differences were considered significant at the 95% confidence level ($p < 0.05$).

Supplemental References

Kannouche, P., Broughton, B. C., Volker, M., Hanaoka, F., Mullenders, L. H., & Lehmann, A. R. (2001). Domain structure, localization, and function of DNA polymerase eta, defective in xeroderma pigmentosum variant cells. *Genes & Development, 15*(2), 158-172.

Zhao, H., Rybak, P., Dobrucki, J., Traganos, F., & Darzynkiewicz, Z. (2012). Relationship of DNA damage signaling to DNA replication following treatment with DNA topoisomerase inhibitors camptothecin/topotecan, mitoxantrone, or etoposide. *Cytometry.Part A : The Journal of the International Society for Analytical Cytology, 81*(1), 45-51. doi:10.1002/cyto.a.21172 [doi]